

Evolution of K -means solution landscapes with the addition of dataset outliers and a robust clustering comparison measure for their analysis

L. Dicks^{1,2} and D. J. Wales^{1, a)}

¹⁾ *Yusuf Hamied Department of Chemistry, Lensfield Road, Cambridge CB2 1EW, United Kingdom*

²⁾ *IBM Research Europe, Hartree Centre, Sci-Tech Daresbury, United Kingdom*

(Dated: 27 June 2023)

The K -means algorithm remains one of the most widely-used clustering methods due to its simplicity and general utility. The performance of K -means depends upon location of minima low in cost function, amongst a potentially vast number of solutions. Here, we use the energy landscape approach to map the change in K -means solution space as a result of increasing dataset outliers and show that the cost function surface becomes more funnelled. Kinetic analysis reveals that in all cases the overall funnel is composed of shallow locally-funnelled regions, each of which are separated by areas that do not support any clustering solutions. These shallow regions correspond to different types of clustering solution and their increasing number with outliers leads to longer pathways within the funnel and a reduced correlation between accuracy and cost function. Finally, we propose that the rates obtained from kinetic analysis provide a novel measure of clustering similarity that incorporates information about the paths between them. This measure is robust to outliers and we illustrate the application to datasets containing multiple outliers.

Keywords: K -means, clustering, outliers, landscapes, topography, cluster comparison

^{a)}Electronic mail: dw34@cam.ac.uk

I. INTRODUCTION

Clustering is ubiquitous in data analysis and, consequently, many diverse clustering methods have been developed. Amongst the most popular is the hard, partitional K -means algorithm.¹ The popularity of K -means stems from its efficiency, algorithmic simplicity, and its ability to produce clusterings in agreement with more complex and expensive algorithms.^{2,3} K -means clusters a given dataset into a prespecified number of clusters, K . For some given initial cluster positions, K -means produces a valid clustering solution by minimising the sum-of-squares cost function until a local minimum is attained. The cost function surface is non-convex and can support many local minima, which correspond to clusterings of varying quality. The number of local minima for the K -means cost function can be vast, and enumeration is impossible for all but trivial cases.⁴

Many schemes for initialising cluster centres have been proposed, which are usually repeatedly applied and, after minimisation of each initial position, the best clustering solution is retained. Many popular initialisation schemes use uniform random samples of the data.⁵⁻⁷ Such methods have a low computational cost, allowing many uncorrelated initial cluster positions to be generated. More complex initialisation schemes draw non-uniform data samples,⁸⁻¹⁰ or pair with other algorithms, such as hierarchical clustering,¹¹ or principal component analysis.¹² These schemes generally have a greater computational cost, but produce local minima of higher quality, allowing fewer distinct initialisations to be considered. Additionally, it is possible to use known solutions to guide future searching, rather than generating uncorrelated trials, and K -means has been paired with genetic algorithms,¹³⁻¹⁵ Monte Carlo-style schemes,¹⁶ and various other optimisation algorithms.¹⁷⁻²¹

The relative performance of all the above methods depends heavily on the dataset structure and the number of clusters.²²⁻²⁵ The effect of dataset structure on K -means performance is encoded by the cost function topography, as the ability of initialisation schemes to locate low-valued K -means minima depends upon the organisation of the solution space. The cost function can be coarse-grained in terms of the local minima and the transition states that connect them, as in the energy landscape framework.²⁶ The structure, thermodynamics, and kinetic properties of physical systems can be described from these stationary points, and we have recently extended this approach to explore the structure of the K -means cost function.^{27,28}

The dependence of clustering accuracy on dataset structure means that datasets are frequently modified prior to clustering to change the structure to favour higher accuracy.²⁹ This preprocessing commonly includes removal of outliers, defined as data points that differ significantly from the rest, which can badly degrade the quality of clustering that is achievable.^{30,31} Hence care is often taken to identify, and remove, outliers prior to clustering. However, there are various methods to make K -means more robust to outliers.^{9,32–36} Clustering itself can reveal outliers, and there are many examples of outlier detection during clustering.^{15,37–39} The effect of outliers on clustering accuracy is well studied, but the effect they have on the organisation of the solution space is unknown, and this is the question we address in this contribution.

We first describe the algorithms of the energy landscape approach, and the extensions required to explore cost function surfaces. Using this framework we analyse the change in the K -means solution space that results from the presence of dataset outliers, and for two datasets we find that the landscape becomes more funnelled. Subsequently, we determine the properties of clustering solutions using kinetic analysis to further examine the nature of the funnelling. Lastly, we propose the use of metrics based upon rates as a robust cluster comparison measure that will be especially useful in describing global optimisation properties.

II. METHODS

A. Local minima

The K -means algorithm aims to minimise the sum-of-squares cost function,

$$J(\boldsymbol{\mu}) = \sum_{i=1}^N \sum_{k=1}^K r_{ik} \|\mathbf{x}_i - \boldsymbol{\mu}_k\|^2. \quad (1)$$

\mathbf{x} is an $(N_f \times N)$ -dimensional matrix that contains the N data points, each of N_f features. $\boldsymbol{\mu}$ contains the coordinates of all K clusters. Each individual data point and cluster are denoted by the N_f -dimensional vectors \mathbf{x}_i and $\boldsymbol{\mu}_k$, respectively. For any given $\boldsymbol{\mu}$, data points are assigned to the nearest cluster centre in Euclidean distance according to

$$r_{ik} = \begin{cases} 1, & \text{if } k = \min_j \|\mathbf{x}_i - \boldsymbol{\mu}_j\|^2, \\ 0, & \text{if otherwise.} \end{cases} \quad (2)$$

r_{ik} is the element of the cluster assignment matrix \mathbf{r} that denotes the assignment of data point i to cluster k .

The cost function, from any given cluster positions, can be locally minimised using Lloyd’s algorithm.¹ Initial cluster coordinates were generated using uniform random points drawn within the range of the dataset in each feature. This inefficient initialisation scheme was chosen to capture both poor and good clustering solutions, as we aim to explore the complete solution space. 10^6 initial cluster positions were generated, and subsequently minimised. Repeated minima were removed, along with those containing empty clusters.

There are a variety of metrics for evaluating the clusterings generated by K -means. Without known data point assignments, as is common in exploratory data analysis, internal metrics can assess clustering quality. Internal metrics use properties of the resulting clusters, such as their compactness and separation. The central internal metric within K -means is the cost function, which gives the within-cluster variance. However, various other internal metrics have been proposed.^{40–42}

In contrast, external metrics measure the similarity of a clustering to a given reference. For labelled datasets we refer to the known partitioning as the ground truth clustering. These ground truth labels are a common reference, in which case we measure the clustering accuracy. Popular external metrics can be based upon cluster matchings,^{43–45} information theory,⁴⁶ or meta-clusters.⁴⁷ We use the adjusted Rand index (ARI)^{43,44} throughout this work, which is described in detail in the SI. The adjusted Rand index ranges from -1 to 1 , with a value of 1 indicating perfect agreement of two clusterings, and 0 indicating the similarity expected between two random clusterings. Values less than 0 indicate a lower similarity than expected for random clusterings.

B. Transition states

For a detailed description of the methodology we employ to explore the K -means cost function topography we refer readers to Ref. 27. A brief summary is presented here.

Transition states provide the lowest barrier in the intermediate region of a surface between one minimum and another and, therefore, provide valuable information about the organisation. There are no transition states, defined as Hessian index one saddles,⁴⁸ on K -means cost function surfaces.²⁷ However, minimum-energy crossing points (MECPs), which lie at

the minimum of an intersection seam between two quadratics defined by different cluster assignments, can be used as transition states in the present context. At all points on a seam the Hessian is undefined, but an MECP can have the correct curvature as a maximum in the direction orthogonal to the intersection seam, and a minimum with respect to all directions along the intersection seam.

Most transition state location algorithms^{49–51} require a function with smooth derivatives, which is not the case for K -means. Instead, we employ a penalty-constrained MECP optimisation algorithm.⁵² Location of an MECP between a pair of cluster assignments, $\mathbf{r}^{(1)}$ and $\mathbf{r}^{(2)}$, which differ in a single data point assignment, can be achieved through minimisation of a surrogate function,

$$F_+(\boldsymbol{\mu}, \mathbf{r}^{(1)}, \mathbf{r}^{(2)}, \sigma, \alpha) = \frac{1}{2} \left(J^{(1)} + J^{(2)} \right) + \sigma \left(\frac{\left(J^{(1)} - J^{(2)} \right)^2}{\|J^{(1)} - J^{(2)}\| + \alpha} \right). \quad (3)$$

$J^{(j)} = J(\boldsymbol{\mu}, \mathbf{r}^{(j)})$ is the K -means cost function, evaluated at cluster position $\boldsymbol{\mu}$, assuming a fixed cluster assignment $\mathbf{r}^{(j)}$. σ and α are parameters that determine the increase in cost function away from the intersection seam, and smooth the surface to avoid a discontinuity there, respectively. $\alpha = 0.02$ and $\sigma = 30$ were used throughout this work, which produced a difference between the cost function evaluated under cluster assignments $\mathbf{r}^{(1)}$ and $\mathbf{r}^{(2)}$ of $\mathcal{O}(10^{-4})$. This difference was sufficiently small for our application, and permitted $\mathcal{O}(10^5)$ transition state location attempts, but the intersection seam can be found to progressively higher accuracy by reminimising F_+ with small increments applied to σ . Minimisations were performed using a customised L-BFGS algorithm.^{53,54}

The minimum of F_+ , our approximation to the MECP, was then evaluated on J to give the cost function at the transition state between clusterings $\mathbf{r}^{(1)}$ and $\mathbf{r}^{(2)}$. Transition states have two connected minima, found by following (approximate) steepest-descent paths beginning in the forwards and backwards direction of the eigenvector corresponding to the unique negative Hessian eigenvalue. For K -means transition states the required eigenvector must be determined from an alternative function. Here we use Eq. (3) with subtraction, rather than addition, of the second term. The function, denoted F_- , penalises the two quadratics when they are similar in value and has the desired negative curvature in the direction perpendicular to the intersection seam. We evaluate the Hessian on the F_- surface, at the minimum of F_+ , to find the negative eigenvalue and its corresponding eigenvector.

C. Building a stationary point network

We have summarised the methodology for finding transition states between neighbouring minima, but to connect a large number of minima we need a scheme to select appropriate pairs for transition state searches. Pairs are selected using a distance-based criterion,⁵⁵ which finds the lowest-valued minimum not currently connected to the global minimum by any sequence of transition states and connected minima, and selects the nearest clustering solution in Euclidean distance that is connected to the global minimum.

For each chosen pair of minima, we do not directly attempt a transition state search, as they may be distant in cluster assignment. Instead, we construct a linear path composed of discrete, equally-spaced cluster positions, referred to as images. The number of images is adapted such that the cluster assignment between any two adjacent images differs by only a single data point, and at such a change in cluster assignment, a transition state search is attempted. F_+ is constructed using the differing cluster assignments of the two images, and a minimisation is started from the first image. If a valid MECP is found we compute the Hessian on F_- and identify the connected minima by LBFGS minimisation. The process is repeated for all differing pairs of images, and the valid transition states are added to a stationary point database, along with their connectivity.

The aim of successive transition state searches is to produce a fully connected set of minima, where it is possible to move between any pair via a series of transition states and connected minima (a discrete path^{56,57}). The repeated application of the distance-based criterion metric to select minima leads to efficient growth of the global minimum connections until all minima are connected. The resulting database of minima and transition states can be represented as a weighted graph, in which minima are nodes, and all pairs of minima connected by a transition state are joined by an edge weighted by a function of the barrier height. For physical systems, this database corresponds to a kinetic transition network,⁵⁸⁻⁶⁰ which we visualise using disconnectivity graphs.^{61,62} Disconnectivity graphs illustrate the minima and the barriers separating them for functions in arbitrary dimensions, as described in Sec. SI.

We construct the analogue of a kinetic transition network for the K -means cost function surface to calculate transition rates between groups of minima. Such rates have no physical analogue, unlike molecular systems, but they nevertheless provide a useful estimate of the

difficulty in moving between different regions of cluster solution space. The rates account for all the intervening barriers in the cost function and all the possible pathways via any number of intervening local minima. These properties are important in understanding the K -means solution space, and contain important additional information that is not present in distance calculations of either cluster positions or assignments.

We compute the rate constant between two minima that are directly connected by a transition state, using the analogue of unimolecular rate theory.^{63,64} The vibrational density of states that appears in this elementary rate theory is set to unity for our K -means applications. The description of global kinetics for a complete network is based upon the combination of the rates of these individual steps, and the graph transformation algorithm^{65,66} was used to calculate all the overall rates reported in this work. We also extract the fastest path, when intervening minima are considered in steady state, using Dijkstra’s algorithm⁶⁷ with suitable edge weights.⁵⁶

The temperature parameter strongly affects the observed pathways and rates. Higher temperatures lead to faster rates, and pathways that contain larger barriers. Each cost function landscape was analysed at a fictitious temperature that produces observed rates in the range between $\mathcal{O}(10^{-6}) - \mathcal{O}(10^{-3})$, which ensures that we favour pathways with small barriers, and see a clearer separation in rates. The cost function landscape itself is independent of temperature.

D. Datasets

We construct K -means landscapes for variations of two labelled datasets: Fisher’s *Iris* dataset⁶⁸ and the glass identification dataset,⁶⁹ both taken from the UCI machine learning data repository.⁷⁰ Fisher’s *Iris* dataset contains 150 data points of four features each. There are fifty measurements of each of the three *Iris* species: *Virginica*, *Versicolor* and *Setosa*. The *Setosa* data points form a clearly-separable cluster, but measurements of the *Versicolor* and *Virginica* species overlap, and cannot be separated by the K -means algorithm.

The glass dataset contains 214 data points separated into six clusters of uneven populations. The dataset has nine features, which exhibit uneven ranges that vary by two orders of magnitude. The ground truth clusters have significant overlap, and the accuracy achievable by K -means is limited for this dataset.

Outliers were sequentially added to both datasets, four to the *Iris* dataset and three to the glass identification dataset. The addition of each successive outlier produced a distinct dataset, giving four *Iris* datasets with an increasing number of outliers. Outliers were placed distant from both the original data points and any existing outliers. The distance between each outlier and the mean of the overall data was not constrained, but is similar for all outliers. The coordinates were selected at random, and are given in Tables SI and SII.

III. RESULTS

Outliers modify K -means clustering to produce two alternative types of solutions:

1. The outlier belongs to a cluster containing no data points from the original dataset.

There remain only $K - O$ clusters to represent the original dataset, where O is the number of outlier clusters. K -means performance is degraded due to poorer partitioning of the original data, and the degradation is greater when the original dataset is composed of K well-separated clusters with little overlap.

2. The outlier belongs to a cluster containing some original data points.

If an outlier does not belong to its own cluster then it must be accommodated in a cluster containing original data points. The outlier may skew the cluster centre a significant distance away from the mean of the original data points, due to its remote position.

The two outlier solutions distinguished above can be used to understand the structure of the clustering solutions within K -means landscapes. For datasets with multiple outliers, each can correspond to one of the two cases, and we provide a classification of the possible structures in Fig. 1.

The structure type, in our specified scheme, is independent of the outlier performing the function. For example, we do not consider which outlier corresponds to its own cluster, giving four options for structure type 1 in a dataset containing four outliers. Each different type 1 solution will have different values of the cost function depending upon where the outlier lies in relation to the original data. However, the scheme remains valuable for understanding the relevant structure of the clusterings.

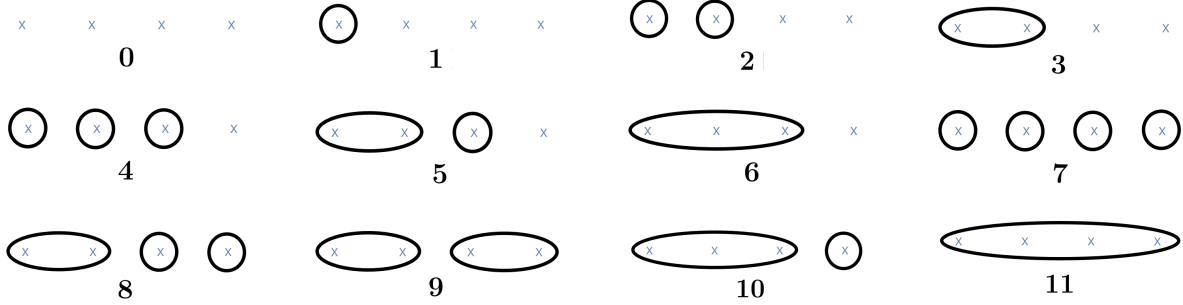


FIG. 1. The structure type scheme used to distinguish clusterings containing outliers. Each cross represents an outlier in the K -means landscape, irrespective of position in space. Circles surrounding one or more outliers indicate membership of a distinct cluster with no original data points. All other outliers are incorporated into clusters with original data points. The scheme is shown for four outliers, but the ordering remains the same for datasets with fewer than four.

A. Cost function topography

The topography of the solution space is central to global optimisation of all machine learning algorithms, and for K -means it determines the ease of locating the optimal clustering. First, we visualise the global structure of the solution space, and describe its properties with reference to global optimisation. Subsequently, we use kinetic analysis to further explore the intermediate regions of solution space, and finally address the properties of the clustering solutions.

1. *Disconnectivity graphs*

We present K -means landscapes, visualised using disconnectivity graphs, for Fisher’s *Iris* dataset ($K = 3$ and $K = 6$) and the glass identification dataset ($K = 6$) prepared with an increasing number of outliers in Figs. 2, 3 and 4, respectively. The minima are coloured according to structure type as specified in the previous section. Despite the large increase in the cost function range across K -means landscapes with additional outliers, there is little change in the barrier heights between transition states and their connected minima, which generally remain very small throughout. Furthermore, the barriers to the global minimum, which can involve pathways containing many minima and transition states, also remain small for the vast majority of minima. This structure produces a strong funnelling in the

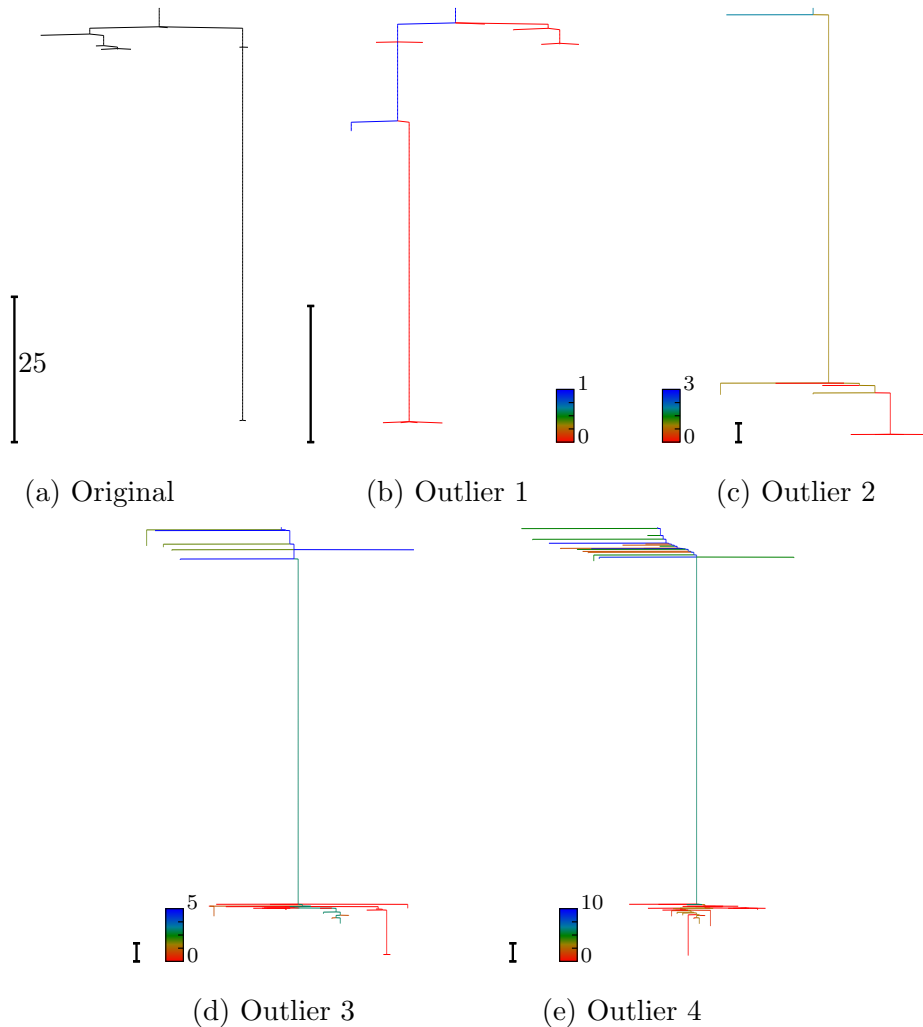


FIG. 2. K -means landscapes for Fisher’s *Iris* dataset with $K = 3$ and an increasing number of outliers. The scale bar represents the same cost function range in all plots. Minima are coloured according to the scheme, given in Fig. 1, for distinguishing different types of K -means solutions.

cost function surface. Single-funnel landscapes⁷¹ are characterised by efficient relaxation to a well-defined global minimum, as for biomolecules that have evolved to perform a single function.

Despite the largely funnelled organisation of minima, there remain regions of solution space separated from the global minimum by significant barriers in all the K -means landscapes. These regions of the surface are referred to as kinetic traps, because they slow relaxation to the global minimum in physical systems, and impede global optimisation algorithms.^{72,73} The kinetic trap regions tend to retain a strong local funnelling to their lowest minimum, and constitute regions of solution space that are distinct from the global

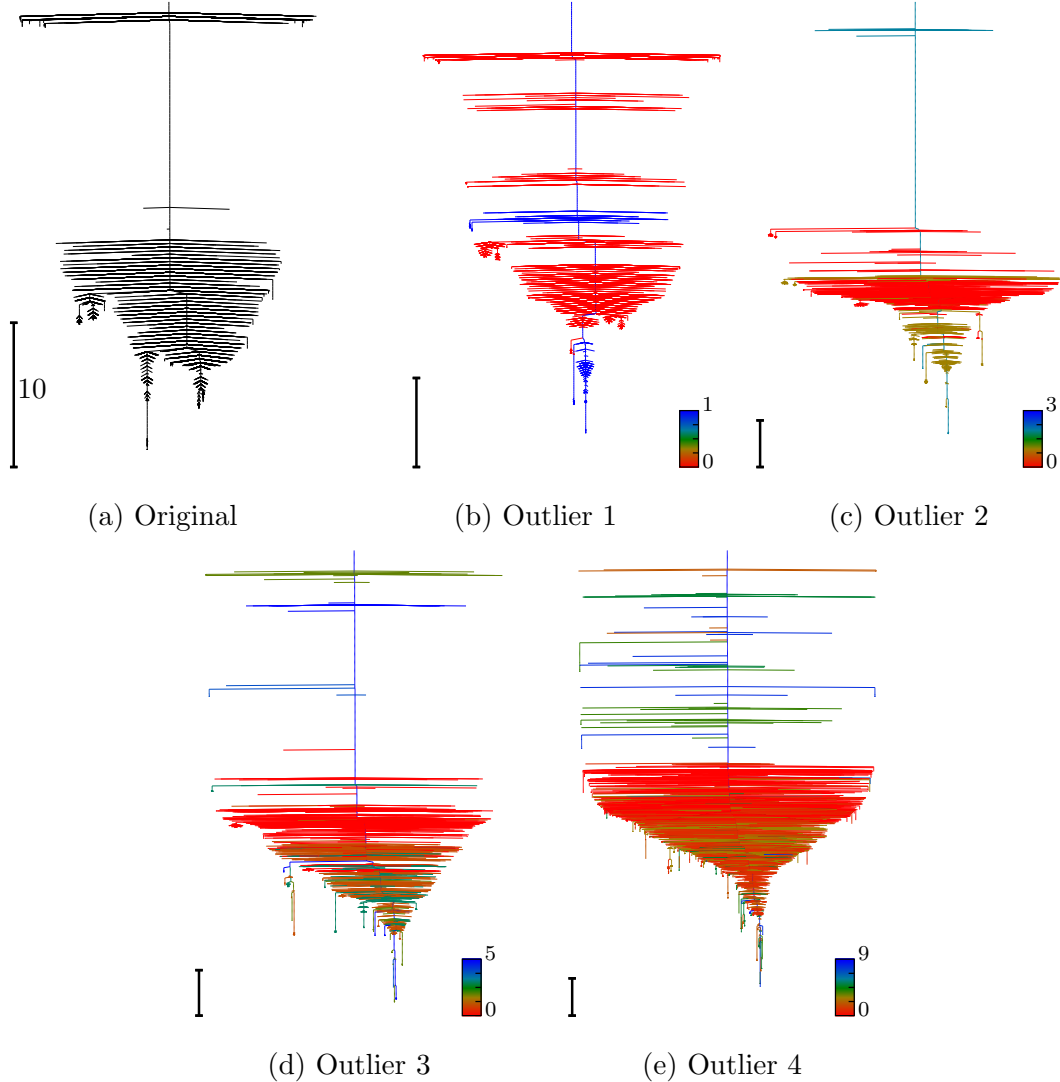


FIG. 3. Disconnectivity graphs showing the K -means solution landscapes for variants of Fisher’s *Iris* dataset with six clusters. The scale bar represents the same cost function range in each case, and minima are coloured according to the scheme given for distinguishing different types of K -means solutions.

minimum.

The number of kinetic traps is generally comparable in K -means landscapes corresponding to datasets with more outliers, despite the large increase in the number of different structure types available to the clustering. However, as the number of outliers increases there is a smaller proportion of minima associated with these kinetic traps. Therefore, with the small barriers retained for many minima, and fewer minima in kinetic traps, the landscapes appear increasingly funnelled for a greater number of outliers.

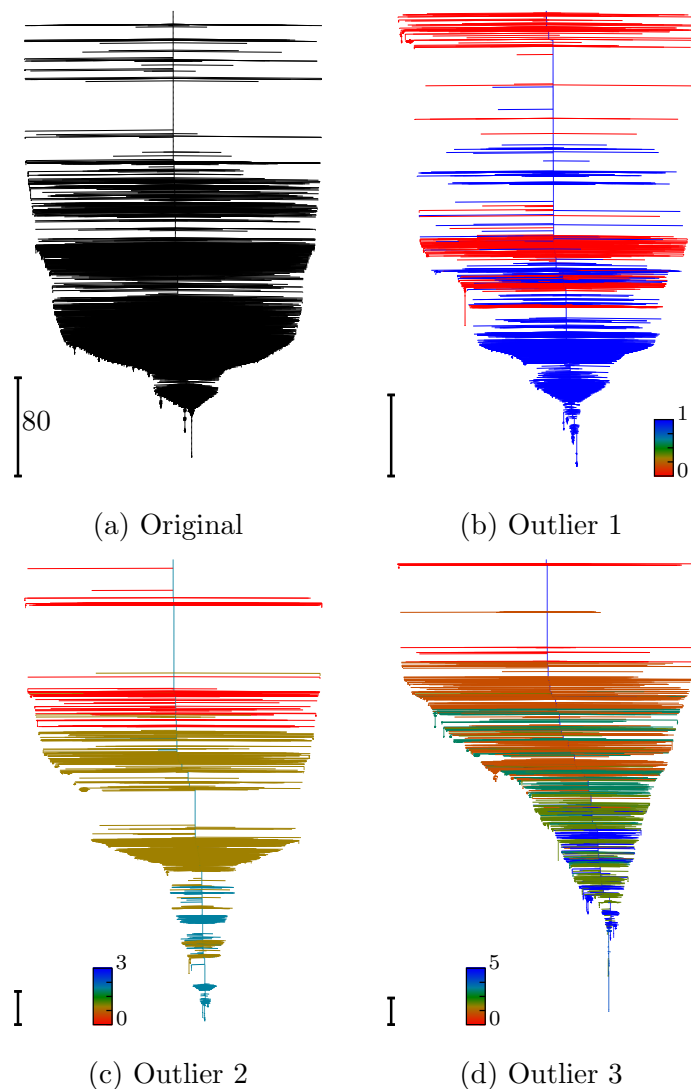


FIG. 4. K -means solution landscapes for the glass identification dataset, and variations with additional outliers. Minima are coloured according to the structure types specified in Fig. 1. The scale bar corresponds to the same cost function range in each case.

2. Frustration

One important quantification of landscape funnelling is the frustration, which we diagnose using the Shannon entropy,⁷⁴ which has previously been used for both molecular energy landscapes⁷⁵ and K -means landscapes.²⁸ Increasing frustration values are associated with a reduction in landscape funnelling due to more kinetic traps, larger barriers, and more alternative low-valued solutions. Greater frustration highlights an increased challenge for global optimisation and an increase in the number of different regions of solution space that

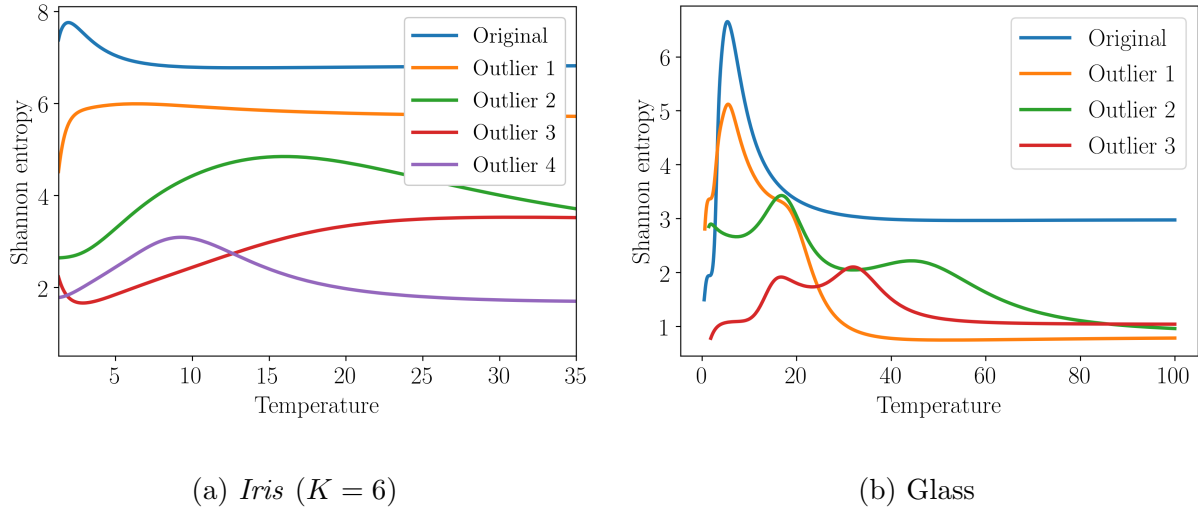


FIG. 5. The Shannon entropy, used as a measure of landscape frustration, calculated for each solution landscape from the *Iris* and glass datasets. The entropy quantifies the complexity of the cost function surface as a function of the fictitious temperature, where $k_{\text{B}}T$ has the same units as the cost function. Local minima with higher cost functions are progressively occupied as the temperature increases.

need to be considered during clustering.

Shannon entropy profiles are shown for the *Iris* and glass landscapes in Fig. 5. The frustration metric is not presented for the *Iris* dataset with three clusters, due to the limited number of minima. For both landscapes we see a smooth decrease in frustration as the number of outliers increases. Therefore, the stronger funnelling seen in the disconnectivity graphs is further reflected by the frustration metric, which demonstrates that the addition of outliers drives funnelling of the landscapes. Furthermore, for the glass landscapes we observe multiple peaks in the frustration profiles. These features correspond to strong fluctuations in either the degeneracy of minima, or the size of their respective basins of attraction, for minima at progressively higher cost function. Such fluctuations hint at the appearance of distinct types of clustering becoming available, which would otherwise be difficult to discern without analysing all the data point assignments.

3. *Kinetic analysis*

Disconnectivity graphs provide a representation of the overall barriers, but the application of kinetic analysis produces a more detailed view of the solution space organisation. Rates and pathways calculated between specified minima include contributions from both the intermediate barriers and minima that describe the space between solutions. We separate out two types of pathways to the global minimum, those starting from minima within the main funnel and those from kinetic traps.

For the majority of minima not within kinetic traps, the small barriers that need to be overcome to reach the global minimum permit different structure types to lie on a funnelled landscape. However, these small downhill barriers do not imply that the pathways between two different structures and the global minimum are similar. We compute the pathways from all different structure types embedded in the funnel to the global minimum to probe the landscape between the optimal solution and sub-optimal solutions. The cost function profiles of the fastest pathways between each set of minima are visualised in Fig. 6 for the *Iris* datasets, and Fig. S1 for the glass datasets.

The pathways reveal repeated features, such as short plateau regions separated by sharp decreases in cost function. These features are retained as outliers are added, and show that the solution space remains composed of many shallow funnelled regions within a broad funnel that encompasses almost all the space. The shallow funnels correspond to a set of minima that belong to the same underlying partitioning or structure type and differ only in the assignment of a small number of data points, leading to small changes in cost function when displacing the cluster positions between them. The overall funnel contains all these regions corresponding to different partitioning and structure types. The sharp changes in cost function arise due to regions between partitionings and structure types that do not support any solutions, leading to long minimisation pathways that result in a significant reduction in J .

Outliers permit longer pathways within a funnel, because there are additional alternative structure types. Similar structure types retain short pathways, even with four outliers, but a greater proportion of transitions within the funnel pass through more intermediate shallow funnels to attain the global minimum. The difference in these short and long pathways are highlighted in Figs. S2 and S3 for the *Iris* dataset with four outliers.

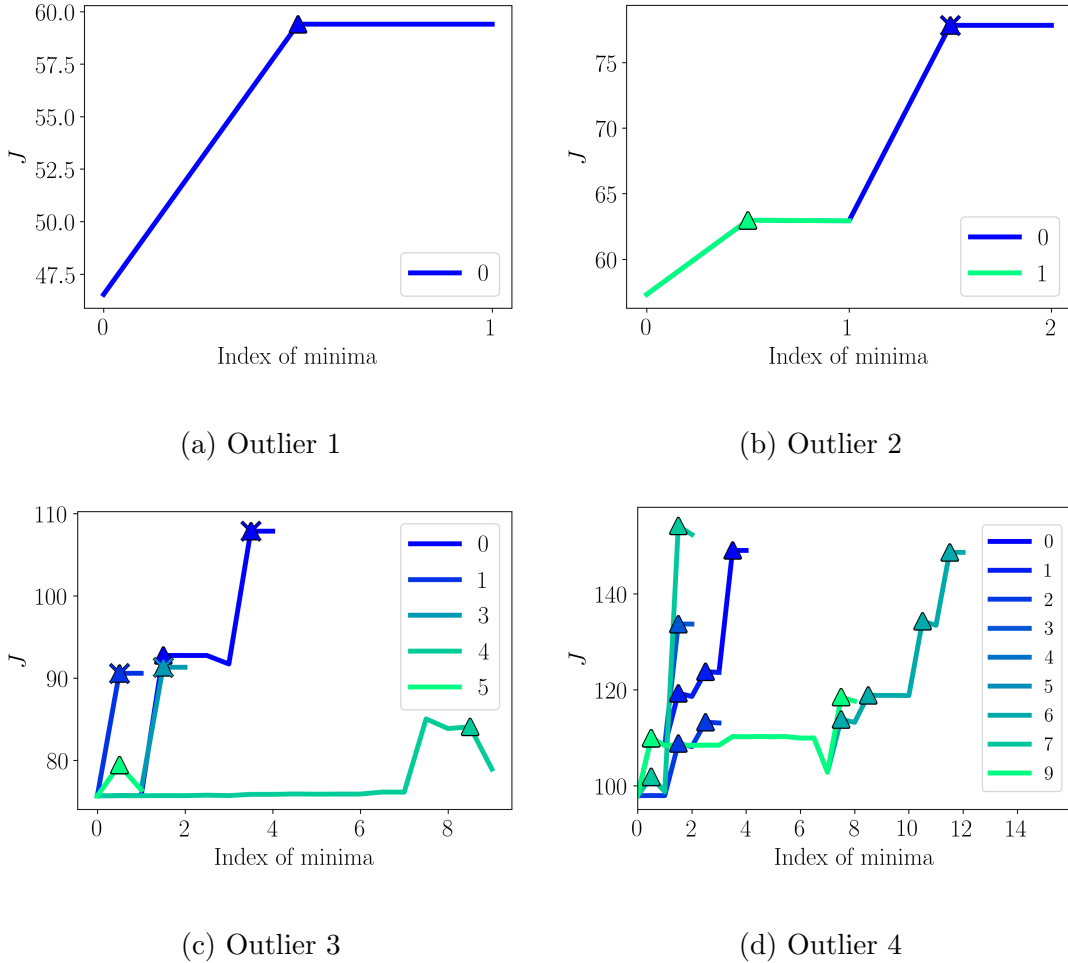


FIG. 6. The fastest paths from minima with a given structure type to the global minimum for the *Iris* dataset with $K = 6$, and its variations with outliers. All stationary points on the pathway are shown, and changes in structure type and partition are denoted by triangles and crosses on transition states, respectively.

For minima in kinetic traps there are much more significant barriers to the global minimum along the pathways, as shown in Fig. 7 for the *Iris* landscape, and Fig. S4 for the glass dataset. These large barriers are associated with changes in partition and structure type. Intermediate regions of the pathways still show shallow regions that indicate rearrangement within a partition or structure type to allow for the larger structural transitions. The glass pathways are much shorter than those for the *Iris* dataset, and have fewer large barriers, which is likely due to the selected kinetic traps having the same structure type as the global minimum for all but the Outlier 3 landscape. The pathways on other landscapes still contain large barriers, and these are likely due to changes in partition, which we cannot diagnose

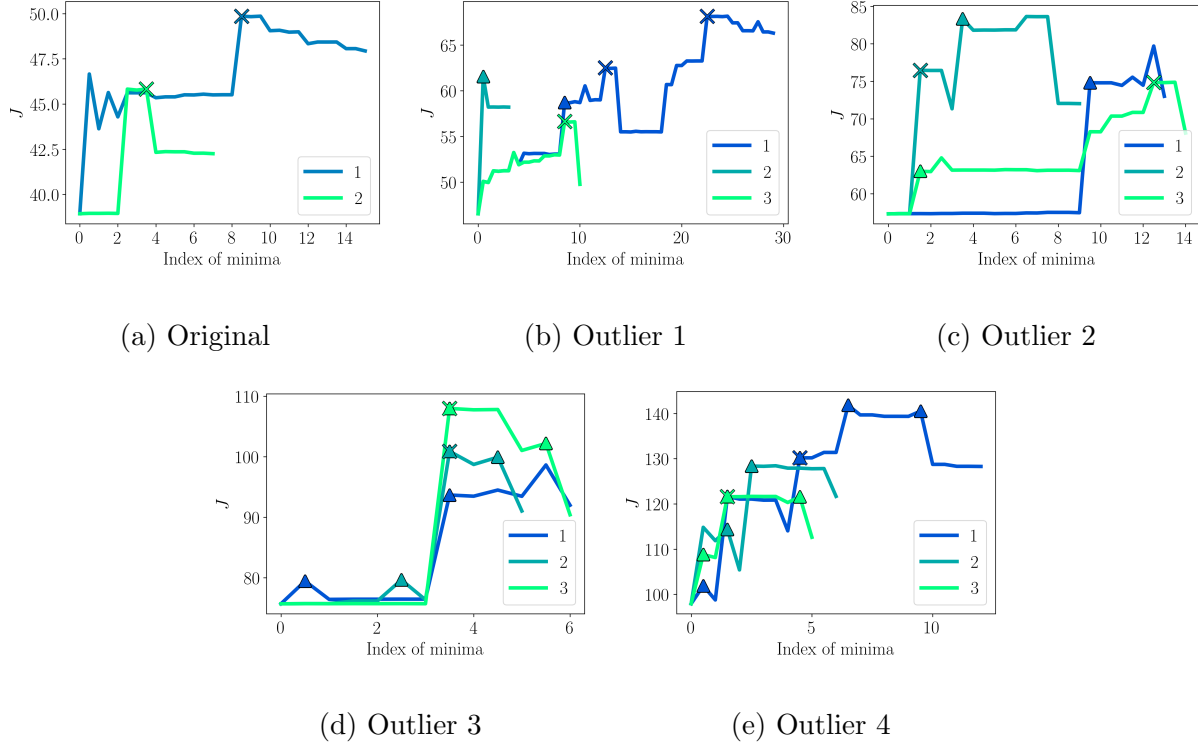


FIG. 7. The fastest paths between minima corresponding to the kinetic traps given in Fig. S5 and the global minimum for the *Iris* dataset with $K = 6$, and variants with additional outliers. Paths are represented by minima, at integer values along the horizontal axis, and the transition states between them. These minima and transition states are connected by straight lines to guide the eye. Changes in structure type are denoted by triangles, and changes in partition by crosses, placed on the transition states that connect the two differing minima.

straightforwardly.

4. Clustering solution properties

For a complete picture of the solution space it is important to determine the properties of clustering solutions, such as accuracy. If minima lower in cost function do not have higher accuracy then global optimisation may not produce the best clusterings. The cost function favours solutions that have low within-cluster variance, which may not necessarily correlate with high accuracy. Accuracy is here computed as the ARI between the ground truth cluster labels and the cluster labels of a given minimum. The accuracy distribution of the minima is given in Fig. 8, and the disconnectivity graphs coloured by accuracy are given in Figs. S7

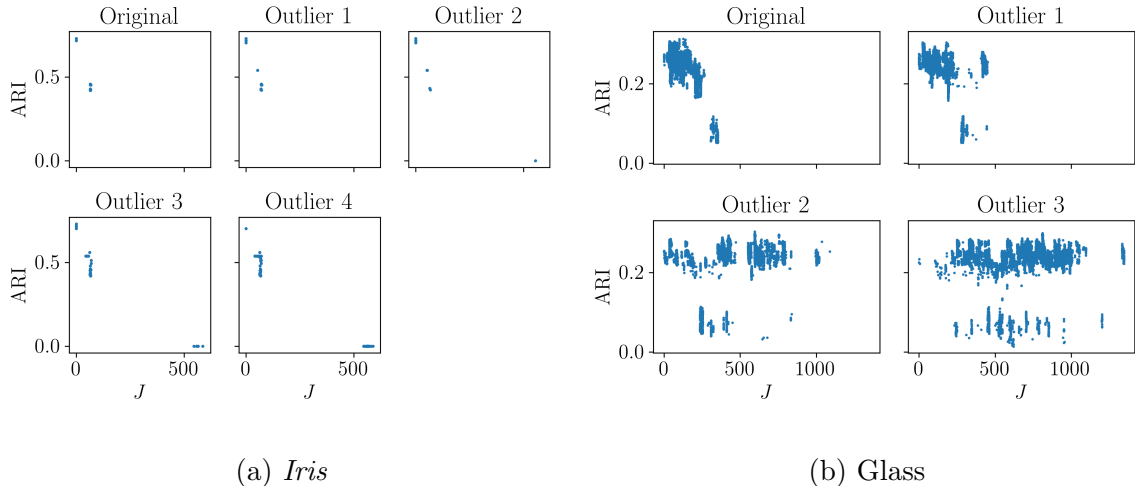


FIG. 8. The distribution of clustering solution accuracy for the glass and *Iris* dataset ($K = 3$). The accuracy was quantified using the adjusted Rand index (ARI) between each clustering and the ground truth labels.

and S8.

For the *Iris* dataset with $K = 3$ the cost function correlates strongly with clustering accuracy, due to the small amount of overlap. The highest achievable accuracy is 0.730, as the K -means algorithm is unable to separate the *Versicolor* and *Virginica* clusters. There is little reduction in the best accuracy on addition of increasing outliers, because the global minimum accommodates the outliers by appending them to existing clusters (Fig. S9), which results in little change in the cluster boundaries from the original dataset. However, for landscapes of two outliers or more we see low-valued solutions that correspond to one outlier cluster; the *Iris* dataset can be well represented with two clusters due to the overlap of *Versicolor* and *Virginica* data points.

The accuracy distribution of the glass identification dataset exhibits different behaviour. This dataset contains significant overlap and, although the accuracy still generally decreases with increasing cost function for the original glass dataset, the K -means cost function is less appropriate for clustering the dataset. The relationship between the cost function value and accuracy becomes weaker with a growing number of outliers, and at three outliers the accuracy has no relation to the cost function. Both the highest attainable accuracy and the accuracy of the global minimum decrease with additional outliers. The most accurate clustering moves to a higher cost function value, relative to the global minimum, and the

most accurate clustering is not the global minimum in any landscape. With additional outliers the most accurate solutions appear repeatedly at different values of the cost function.

For the *Iris* dataset with $K = 6$ we cannot evaluate the accuracy, but we can rationalise the significant kinetic traps in the original *Iris* landscape by equating them to different partitionings of the six K -means clusters amongst the three underlying clusters. Partitionings remain useful to understand kinetic traps, but as the number of outliers increases the structure type exerts more control over cost function topography. Partitionings become less clear, as many clusters now incorporate outliers, and a growing number of kinetic traps can be rationalised by a difference in structure type, and not partition. Disconnectivity graphs coloured by partitioning are given for *Iris* datasets with both cluster numbers in Fig. S10, and the different structure types of the global minima are shown in Fig. S11.

B. Rate-based clustering comparison

We propose that the rate computed between clustering solutions can be used as a measure of their distinctness. All current external metrics for comparing clusterings use only the initial and final configurations, but the rates depend on the path between them, including information about the number of intermediate minima and the barriers for cluster displacements. Hence this metric encodes the cumulative change in cluster position and assignment, rather than just the difference between endpoints. It is related to the difficulty in navigating the landscape between two clusterings, providing valuable insight into global optimisation performance for K -means. Moreover, rates implicitly weight the importance of data points by the change they induce in the cost function, which allows a robust measure of cluster distinctness, even in the presence of dataset outliers.

We examine the correlation between rates, cluster position (distance), and cluster assignment (ARI) measure in Fig. 9. The clustering similarity measures were computed between different structure types in all outlier landscapes for the *Iris* dataset with six clusters. The structure types differ in the assignment of outliers, which can be challenging for cluster assignment-based metrics because a few data point label changes produce a large effect. Consequently, we observe a weak positive correlation with the ARI. The distance captures the large distorting effect of the outliers on cluster positions, and we observe a strong correlation with the rate, which therefore also captures the importance of individual data points

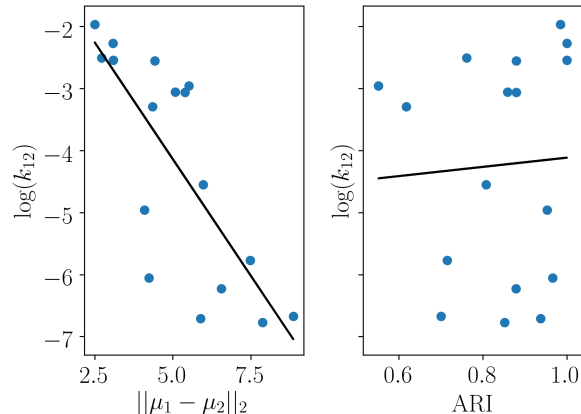


FIG. 9. Correlation between rates, k_{12} , and two other external metrics for cluster comparison: the distance between cluster centres (left) and the ARI (right). The pairs of clusterings are different structure types of the *Iris* datasets containing outliers. The line of best fit is the solid black line.

for cluster distinctness. However, the three metrics probe different features of the clustering distinctness, and there are many examples where the pathway-based measure does not simply relate to the distance. We illustrate the comparative measures alongside the clusterings, in three of the four dimensions, for the same set of minima in Fig. S12.

We compute the rates for various transitions that will affect global optimisation, such as between different structure types and for kinetic traps to the global minimum. These rates reflect the distinctness of various clusterings from the global minimum, and hence report on the difficulty of global optimisation from each starting point. The rates between different structures embedded in the funnel can vary significantly, even for minima with comparable cost functions, as shown in Tables I and SIV. The rates largely correlate with the number of different structure types (or more rarely partitions) that must be visited on the way to reaching the global minimum. The rates remain similar across all outlier numbers when the structure types involve a small number of changes, as the similarity of such structures is retained. However, the rates can be much slower in landscapes with more outliers, due to the greater difference in arrangements of distant structure types. The rearrangement of multiple outliers involves more transition states and intermediate minima, and the rates therefore decrease. The reduction in slowest rate with outliers is much more pronounced for the glass dataset. Furthermore, the rates remain remarkably similar between all structure types, without the large preference for transitions between structures of the same type seen

TABLE I. Transition rates (reduced units) between the set of minima of a given structure type to the global minimum, calculated at an effective temperature of $T = 1.0$ (in reduced units consistent with the cost function). Rates are calculated for the *Iris* dataset with $K = 6$, and those datasets with additional outliers. The dot indicates the structure type of the global minimum.

Type	Outlier 1	Outlier 2	Outlier 3	Outlier 4
0	3.11×10^{-3}	8.82×10^{-4}	2.82×10^{-5}	1.68×10^{-7}
1	.	1.08×10^{-2}	2.78×10^{-3}	1.94×10^{-7}
2		.	.	8.81×10^{-7}
3			8.68×10^{-4}	5.90×10^{-7}
4			5.11×10^{-4}	5.34×10^{-3}
5			2.85×10^{-3}	1.10×10^{-5}
6				2.12×10^{-7}
7				1.11×10^{-3}
8				.
9				1.70×10^{-6}

TABLE II. Escape rates (reduced units) from kinetic traps on the solution landscape for the *Iris* dataset with $K = 6$, and variations with additional outliers. The rates are calculated from the set of minima at the bottom of the kinetic trap to the global minimum, at an effective temperature of $T = 1.0$ (reduced units). The selected kinetic traps are given in Fig. S2. The geometric mean rate for each landscape is given in the final row.

Kinetic trap	Original	Outlier 1	Outlier 2	Outlier 3	Outlier 4
1	3.65×10^{-4}	2.25×10^{-5}	2.64×10^{-4}	3.23×10^{-4}	7.25×10^{-7}
2	1.74×10^{-5}	1.02×10^{-3}	6.55×10^{-8}	3.26×10^{-6}	1.12×10^{-6}
3	-	2.66×10^{-5}	2.20×10^{-5}	2.26×10^{-9}	8.57×10^{-7}
Mean	7.97×10^{-5}	8.48×10^{-5}	7.25×10^{-6}	1.34×10^{-6}	8.86×10^{-7}

in the *Iris* dataset.

The rates between kinetic traps and the global minimum are given in Table II and Table SV for the *Iris* and glass datasets, respectively. These rates generally decrease as the number of outliers increases. The escape rates from different kinetic traps within the same landscape exhibit large fluctuations as a result of the specific features. However, there remains an overall reduction in escape rates and, consequently, escaping kinetic traps becomes more difficult as the number of outliers increases.

IV. CONCLUSIONS

Successful K -means clustering depends on two factors: efficient location of the global minimum (or low-valued minima), and the appropriateness of the cost function, so that low-valued minima are the most accurate. The efficiency of global optimisation is encoded in the organisation of the solution space. We find that these landscapes have a funnelled structure for the datasets we consider with any number of outliers. The degree of funnelling, as quantified using a frustration metric, increases with the number of outliers.

Kinetic analysis reveals that the overall funnel seen in each landscape is composed of many different shallow regions that correspond to different types of structure. These shallow regions of space involve small barriers between different structure types, and they are separated by cluster solution space that does not contain any minima. Therefore, there can be large changes in cost function between these regions associated with long pathways. The number of such structure types increases with the number of outliers, which can result in much longer pathways for navigation of the funnel.

We have introduced kinetic analysis of the K -means landscapes as a novel clustering similarity measure. The rate extends external clustering metrics by incorporating information about pathways between clustering solutions, rather than just the endpoints. Such a measure can quantify the cumulative change in cluster position and assignment, which may be more relevant for rationalising global optimisation performance. We compute rates within the *Iris* and glass datasets to analyse the similarity between different regions of the solution space. We observe that high similarity is conserved between adjacent structure types across all outlier landscapes, but the lowest similarity decreases as the number of outliers increases.

A funnelled surface is usually favourable for global optimisation in physical systems. However, the rates illustrate that it becomes more challenging to both escape kinetic traps, and relax within the main funnel, to locate the global minimum with increasing outliers. There is a sharp increase in the number of ways in which outliers can be accommodated into clusterings as the number of outliers increases, and this increase leads to longer pathways between different regions of space. Therefore, although movement between adjacent structure types remains fast, it becomes more challenging to move about the main funnel between a greater number of structure types. For successful global optimisation runs from distinct starting configurations may be helpful, and an efficient moveset would require

both local perturbations, which optimise cluster boundaries, and larger changes between different structure types by exchanging outliers. However, with an appropriate moveset the single-funnel solution space should allow the global minimum to be located quite efficiently.

The correlation between cost function and accuracy is degraded by the increased number of outliers. The outliers perturb the cluster centre positions, leading to reduced accuracy of the low-valued solutions. Additionally, the increase in the number of structure types produces greater variation in the accuracy throughout the cost function range. Therefore, for datasets containing multiple outliers, obtaining the global minimum does not necessarily give the most accurate clustering solution that K -means can support. Without a clear way to distinguish accurate solutions in cost function it is important to use an internal metric, such as the silhouette coefficient,⁴² to independently rank them. However, except for the case of three outliers in the highly-overlapping glass dataset, we observe that the low-valued region does contain minima of comparable accuracy to the most accurate clustering. Hence locating low-valued minima is useful, but it becomes essential to generate an ensemble of clustering solutions, which can capture the many possible arrangements of the various outliers.⁷⁶

V. SUPPLEMENTARY MATERIAL

See the supplementary material for additional methodological details (S-I and S-III), a description of the datasets used in this work (S-II), and additional figures referenced in this work (S-IV).

VI. ACKNOWLEDGEMENTS

This work was supported by an EPSRC knowledge transfer fellowship. DJW gratefully acknowledges an International Chair at the Interdisciplinary Institute for Artificial Intelligence at 3iA Cote d’Azur, supported by the French government [grant number ANR-19-P3IA-0002], which has provided interactions that furthered the present research project.

REFERENCES

¹S. Lloyd. Least squares quantization in PCM. *IEEE Trans. Inf. Theory*, 28:129–137, 1982.

- ²A. K. Jain, A. Topchy, M. H. C. Law, and J. M. Buhmann. Landscape of clustering algorithms. In *Proc. of the IAPR Int. Conf. Pattern Recognit.*, pages 260–263, 2004.
- ³M. C. P. de Souto, I. G. Costa, D. S. A. de Araujo, T. B. Ludemir, and A. Schliep. Clustering cancer gene expression data: a comparative study. *BMC Bioinform.*, 9:497, 2008.
- ⁴M. Mahajan, P. Nimbhorkar, and K. Varadarajan. The planar K -means problem is NP-hard. *Theor. Comput. Sci.*, 442:13–21, 2012.
- ⁵D. Steinley. Local optima in K -means clustering: what you don’t know may hurt you. *Psychol. Methods*, 8:294–304, 2003.
- ⁶P. S. Bradley and U. M. Fayyad. Refining initial points for K -means clustering. *Int. Conf. Mach. Learn.*, 1:91–99, 1998.
- ⁷V. Faber. Clustering and the continuous K -means algorithm. *Los Alamos Science*, 22:138–144, 1994.
- ⁸D. Arthur and S. Vassilvitskii. k -means++: the advantages of careful seeding. In *Proc. of the 18th Ann. ACM-SIAM Symp. on Discrete Algorithms*, pages 1027–1035, 2007.
- ⁹A. H. Mohammad, C. Vineed, S. Saeed, and J. Z. Mohammed. Robust partitional clustering by outlier and density insensitive seeding. *Pattern Recognit. Lett.*, 30:994–1002, 2009.
- ¹⁰O. Bachem, M. Lucic, S. Hamed Hassani, and A. Krause. Fast and provably good seedings for k -means. In *Proc. of the 30th Int. Conf. on Neural Information Processing Systems*, pages 55–63, 2016.
- ¹¹G. W. Milligan and P. D. Isaac. The validation of four ultrametric clustering algorithms. *Pattern Recognit.*, 12:41–50, 1980.
- ¹²T. Su and J. G. Dy. Another look at non-random methods for initializing K -means clustering. In *Proc. of the 16th IEEE Int. Conf. Tools Art. Intell.*, pages 784–786, 2004.
- ¹³K. Krishna and M. N. Murty. Genetic K -means algorithm. *IEEE Trans. Syst. Man Cybern.*, 29:433–439, 1999.
- ¹⁴P. Fränti. Genetic algorithm with deterministic crossover for vector quantization. *Pattern Recognit. Lett.*, 21:61–68, 2000.
- ¹⁵M. H. Marghny and A. I. Taloba. Outlier detection using improved genetic k -means. *arXiv*, 2014.

- ¹⁶D. J. Hand and W. J. Krzanowski. Optimising K -means clustering results with standard software packages. *Comput. Stat. Data Anal.*, 49:969–973, 2005.
- ¹⁷A. Hatamlou, S. Abdullah, and H. Nezamabadi-pour. A combined approach for clustering based on k -means and gravitational search algorithms. *Swarm Evol. Comput.*, 6:47–52, 2012.
- ¹⁸M. Yao, Q. Wu, J. Li, and T. Huang. k -walks: clustering gene-expression data using a k -means clustering algorithm optimised by random walks. *Int. J. Data Mining Bioinf.*, 16:121–140, 2016.
- ¹⁹P. Das, D. K. Das, and S. Dey. A modified bee colony optimization (MBCO) and its hybridization with k -means for an application to data clustering. *Appl. Soft Comput.*, 70:590–603, 2018.
- ²⁰V. N. Manju and A. L. Fred. AC coefficient and K -means cuckoo optimisation algorithm-based segmentation and compression of compound images. *IET Image Process.*, 12:218–225, 2018.
- ²¹H. Xie, L. Zhang, C. P. Lim, Y. Yu, C. Liu, H. Liu, and J. Walters. Improving K -means clustering with enhanced firefly algorithms. *Appl. Soft Comput.*, 84:105763–105785, 2019.
- ²²D. Steinley and M. J. Brusco. Initializing K -means batch clustering: a critical evaluation of several techniques. *J. Classif.*, 24:99–121, 2007.
- ²³M. Filippone, F. Camastra, F. Masulli, and S. Rovetta. A survey of kernel and spectral methods for clustering. *Pattern Recognit.*, 41:176–190, 2008.
- ²⁴P. Rai and S. Singh. A survey of clustering techniques. *Int. J. Comput. Appl.*, 7:1–5, 2010.
- ²⁵M. E. Celebi, H. A. Kingravi, and P. A. Vela. A comparative study of efficient initialization methods for the K -means clustering algorithm. *Expert Syst. Appl.*, 40:200–210, 2013.
- ²⁶D. J. Wales. *Energy Landscapes*. Cambridge University Press, Cambridge, 2003.
- ²⁷L. Dicks and D. J. Wales. Elucidating the solution structure of the K -means cost function using energy landscape theory. *J. Chem. Phys.*, 156:054109, 2022.
- ²⁸Y. Wu, L. Dicks, and D. J. Wales. Archetypal solution spaces for clustering gene expression datasets in identifying cancer subtypes. *arXiv*, 2023.
- ²⁹L. A. Shalabi, Z. Shaaban, and B. Kasasbeh. Data mining: a preprocessing engine. *J. Comput. Sci.*, 2:735–739, 2006.
- ³⁰L. A. García-Escudero and A. Gordaliza. Robustness properties of k -means and trimmed k -means. *J. Am. Stat. Assoc.*, 94:956–969, 1999.

- ³¹J-S. Zhang and Y-W. Leung. Robust clustering by pruning outliers. *IEEE Trans. Sys. Man Cybern.*, 33:983–999, 2003.
- ³²J. Xu, J. Han, K. Xiong, and F. Nie. Robust and sparse fuzzy K -means clustering. In *Proc. of the 25th Int. Joint Conf. Art. Intell.*, pages 2224–2230, 2016.
- ³³S. Gupta, R. Kumar, K. Lu, B. Moseley, and S. Vassilvitskii. Local search methods for k -means with outliers. In *Proc. of the VLDB Endowment*, pages 757–768, 2017.
- ³⁴S. Huang, Y. Ren, and Z. Xu. Robust multi-view data clustering with multi-view capped-norm k -means. *Neurocomputing*, 311:197–208, 2018.
- ³⁵Š. Brodinová, P. Filzmoser, T. Ortner, C. Breiteneder, and M. Rohm. Robust and sparse k -means clustering for high-dimensional data. *Adv. Data Anal. Classif.*, 13:905–932, 2019.
- ³⁶X. Zhang, Y. He, Y. Jin, H. Qin, M. Azhar, and J. Z. Huang. A robust k -means clustering algorithm based on observation point mechanism. *Complexity*, 2020.
- ³⁷M. B. Al-Zoubi. An effective clustering-based approach for outlier detection. *Eur. J. Sci. Res.*, 28:310–316, 2009.
- ³⁸M. F. Jiang, S. S. Tseng, and C. M. Su. Two-phase clustering process for outliers detection. *Pattern Recognit. Lett.*, 22:691–700, 2001.
- ³⁹Z. Zhang, Q. Feng, J. Huang, Y. Guo, J. Xu, and J. Wang. A local search algorithm for k -means with outliers. *Neurocomputing*, 450:230–241, 2021.
- ⁴⁰J. C. Dunn. Well-separated clusters and optimal fuzzy partitions. *J. Cybern.*, 4:95–104, 1974.
- ⁴¹D. L. Davies and D. W. Bouldin. A cluster separation measure. *IEEE Trans. Pattern Anal. Mach. Intell.*, 1:224–227, 1979.
- ⁴²P. J. Rousseeuw. Silhouettes: a graphical aid to the interpretation and validation of cluster analysis. *Comput. Appl. Math.*, 20:53–65, 1987.
- ⁴³W. M. Rand. Objective criteria for the evaluation of clustering methods. *J. Am. Stat. Assoc.*, 66:846–850, 1971.
- ⁴⁴L. Hubert and P. Arabie. Comparing partitions. *J. Classif.*, 2:193–218, 1985.
- ⁴⁵E. B. Fowlkes and C. L. Mallows. A method for comparing two hierarchical clusterings. *J. Am. Stat. Assoc.*, 78:553–569, 1983.
- ⁴⁶M. Meilă. Comparing clusterings – an information based distance. *J. Multivar. Anal.*, 98:873–895, 2007.

- ⁴⁷F. Cazals, D. Mazaauric, R. Tetley, and R. Watrigant. Comparing two clusterings using matchings between clusters of clusters. *J. Exp. Algorithmics*, 24:1–41, 2019.
- ⁴⁸J. N. Murrell and K. J. Laidler. Symmetries of activated complexes. *Trans. Faraday Soc.*, 64:371–377, 1968.
- ⁴⁹L. J. Munro and D. J. Wales. Defect migration in crystalline silicon. *Phys. Rev. B*, 59:3969–3980, 1999.
- ⁵⁰G. Henkelman, B. P. Uberuaga, and H. Jónsson. A climbing image nudged elastic band method for finding saddle points and minimum energy paths. *J. Chem. Phys.*, 113:9901–9904, 2000.
- ⁵¹B. Peters, A. Heyden, A. T. Bell, and A. Chakraborty. A growing string method for determining transition states: comparison to the nudged elastic band and string methods. *J. Chem. Phys.*, 120:7877–7886, 2004.
- ⁵²B. G. Levine, J. D. Coe, and T. J. Martínez. Optimizing conical intersections without derivative coupling vectors application to multistate multireference second-order perturbation theory (MS-CASPT2). *J. Phys. Chem. B*, 112:405–413, 2008.
- ⁵³J. Nocedal. Updating quasi-Newton matrices with limited storage. *Math. Comput.*, 35:773–782, 1980.
- ⁵⁴D. C. Liu and J. Nocedal. On the limited memory BFGS method for large scale optimization. *Math. Program.*, 45:503–528, 1989.
- ⁵⁵K. Röder and D. J. Wales. Energy landscapes for the aggregation of $A\beta_{17-42}$. *J. Am. Chem. Soc.*, 140:4018–4027, 2018.
- ⁵⁶D. J. Wales. Discrete path sampling. *Mol. Phys.*, 100:3285–3305, 2002.
- ⁵⁷D. J. Wales. Some further applications of discrete path sampling to cluster isomerization. *Mol. Phys.*, 102:891–908, 2004.
- ⁵⁸F. Noé and S. Fischer. Transition networks for modelling the kinetics of conformational change in macromolecules. *Curr. Opin. Struct. Biol.*, 18:154–162, 2008.
- ⁵⁹J. M. Carr and D. J. Wales. Refined kinetic transition networks for the GB1 hairpin peptide. *Phys. Chem. Chem. Phys.*, 11:3341–3354, 2009.
- ⁶⁰D. Prada-Gracia, J. Gómez-Gardeñes, P. Echenique, and F. Falo. Exploring the free energy landscape: from dynamics to networks and back. *PLoS Comput. Biol.*, 5:e1000415, 2009.
- ⁶¹O. M. Becker and M. Karplus. The topology of multidimensional potential energy surfaces: theory and application to peptide structure and kinetics. *J. Chem. Phys.*, 106:1495–1517,

- 1997.
- ⁶²D. J. Wales, M. A. Miller, and T. R. Walsh. Archetypal energy landscapes. *Nature*, 394:758–760, 1998.
- ⁶³H. Eyring. The activated complex and the absolute rate of chemical reactions. *Chem. Rev.*, 17:65–77, 1935.
- ⁶⁴M. G. Evans and M. Polanyi. Some applications of the transition state method to the calculation of reaction velocities, especially in solution. *Trans. Faraday Soc.*, 31:875–894, 1935.
- ⁶⁵S. A. Trygubenko and D. J. Wales. Graph transformation method for calculating waiting times in Markov chains. *J. Chem. Phys.*, 124:234110, 2006.
- ⁶⁶D. J. Wales. Calculating rate constants and committor probabilities for transition networks by graph transformation. *J. Chem. Phys.*, 130:204111–204118, 2009.
- ⁶⁷E. W. Dijkstra. A note on two problems in connexion with graphs. *Numerische Math.*, 1:269–271, 1959.
- ⁶⁸R. A. Fisher. The use of multiple measurements in taxonomic problems. *Ann. Eugen.*, 7:179–188, 1936.
- ⁶⁹I. W. Evett and E. J. Spiehler. Rule induction in forensic science. *Knowl. Based Sys.*, pages 152–160, 1989.
- ⁷⁰D. Dua and C. Graff. UCI machine learning repository, 2017.
- ⁷¹N. D. Socci, J. N. Onuchic, and P. G. Wolynes. Protein folding mechanisms and the multidimensional folding funnel. *Proteins*, 32:136–158, 1998.
- ⁷²J. D. Bryngelson, J. N. Onuchic, N. D. Socci, and P. G. Wolynes. Funnels, pathways, and the energy landscape of protein folding: a synthesis. *Proteins*, 21:167–195, 1995.
- ⁷³J. N. Onuchic, Z. Luthey-Schulten, and P. G. Wolynes. Theory of protein folding: the energy landscape perspective. *Ann. Rev. Phys. Chem.*, 48:545–600, 1997.
- ⁷⁴C. E. Shannon. A mathematical theory of communication. *Bell Syst. Tech. J.*, 27:379–423, 1948.
- ⁷⁵V. K. de Souza, J. D. Stevenson, S. P. Niblett, J. D. Farrell, and D. J. Wales. Defining and quantifying frustration in the energy landscape: applications to atomic and molecular clusters, biomolecules, jammed and glassy systems. *J. Chem. Phys.*, 146:124103, 2017.
- ⁷⁶T. Alqurashi and W. Wang. Clustering ensemble method. *Int. J. Mach. Learn. & Cyber.*, 10:1227–1246, 2019.

Supplementary material – Evolution of K -means solution landscapes with the addition of dataset outliers and a robust clustering comparison measure for their analysis

L. Dicks^{1,2} and D. J. Wales^{1, a)}

¹⁾ *Yusuf Hamied Department of Chemistry, Lensfield Road, Cambridge CB2 1EW, United Kingdom*

²⁾ *IBM Research Europe, Hartree Centre, Sci-Tech Daresbury, United Kingdom*

(Dated: 27 June 2023)

^{a)}Electronic mail: dw34@cam.ac.uk

I. CONSTRUCTING DISCONNECTIVITY GRAPHS

All clustering solutions (local minima) are represented by vertical lines originating at their corresponding cost function value on the vertical axis. For any given cost function threshold, the minima can be separated into groups connected by barriers below the threshold. The overall barrier between any two minima is given by the cost function at the highest transition state on a path between them, which may be one, or more, transition states in length. Starting from a cost function value above the highest-valued minimum we reduce the threshold by regular intervals and separate the minima into disjoint sets, known as superbasins.¹ The vertical lines corresponding to minima join when the cost function threshold is greater than the barrier between them. The horizontal axis is chosen to arrange minima to provide a clear representation of the topography.

II. DATA PREPARATION

For the *Iris* dataset, the outlier coordinates lie outside the range of the original data in at least half the features. In the glass datasets, the outliers lie outside the range of the original data in every dimension.

TABLE I. The position of outliers added to the *Iris* dataset. The values of the features are all given in centimetres. The mean and range are given for the original dataset.

Outlier	Sepal length	Sepal width	Petal length	Petal width
1	9.6	6.0	5.0	4.0
2	2.0	0.1	0.1	2.5
3	6.0	7.0	0.1	4.0
4	1.0	4.0	8.0	0.5
Mean	5.84	3.05	3.76	1.20
Range	4.3–7.9	2.0–4.4	1.0–6.9	0.1–2.5

TABLE II. The coordinates of the outliers added to the glass dataset. Features are provided in the same order as the data taken from the UCI machine learning data repository. The mean and range are given for the original dataset.

Dataset	x_1	x_2	x_3	x_4	x_5	x_6	x_7	x_8	x_9
1	1.3	5.0	7.0	6.0	60.0	9.0	2.0	5.0	3.0
2	1.7	23.0	7.0	7.0	90.0	9.0	21.0	5.0	4.0
3	1.8	4.0	8.0	7.0	85.0	9.0	1.0	5.0	4.0
Mean	1.52	13.41	2.68	1.44	72.65	0.50	8.96	0.18	0.06
Range	1.51–1.53	10.7–17.4	0.00–4.49	0.29–3.50	69.8–75.4	0.00–6.21	5.43–16.2	0.00–3.15	0.00–0.51

III. COMPARING CLUSTERINGS

The Rand index,² compares two partitions using the following ratio

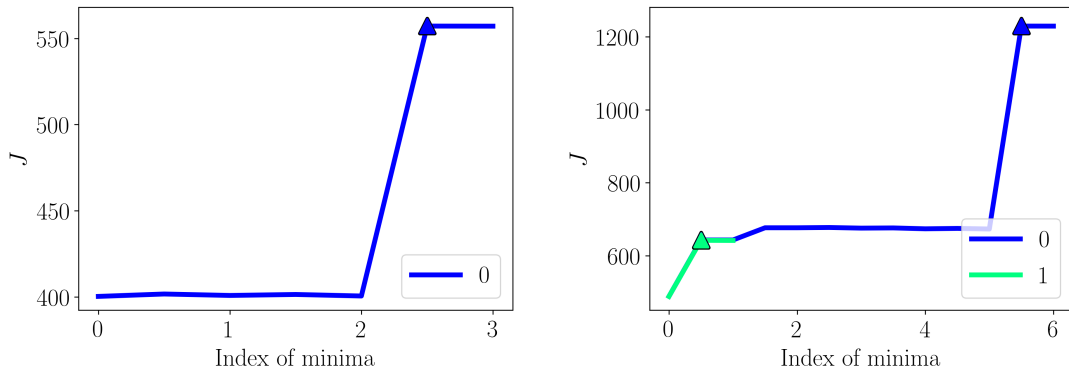
$$RI = \frac{TP + TN}{TP + TN + FP + FN}, \quad (1)$$

where TP, TN, FP, FN are the number of true positives, true negatives, false positives and false negatives, respectively, evaluated over all pairs of data points within a dataset. A true positive occurs when the pair of data points are placed in the same cluster in both the reference and test partitions, and a true negative when they are placed in different clusters in both partitions. False positives and negatives arise when one clustering assigns the two data points to the same cluster, but not the other. A false negative is distinguished by the two data points being assigned to the same cluster in the reference clustering, and for a false positive the data points are in different clusters in the reference.

The Rand index takes values between 0 and 1, with 0 indicating no similarity between the clusterings, and 1 indicating identical clusterings. The Rand index is often close to 1, even with significant differences between the clusterings, because there are often a large number of similar pairwise labellings that arise at random. The Rand index does not account for the similarity expected for random datasets, and the value of the Rand index, calculated for two random clusterings, is greater than zero. The adjusted Rand index³ (ARI) accounts for cluster labels being the same by chance and provides a new baseline, such that expected similarity of all pairwise comparisons within a random model is approximately 0.

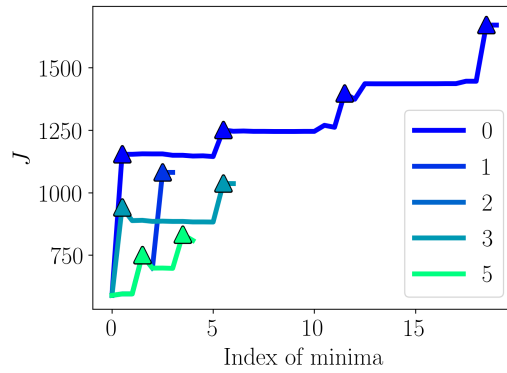
IV. COST FUNCTION TOPOGRAPHY

A. Kinetic analysis



(a) Outlier 1

(b) Outlier 2



(c) Outlier 3

FIG. 1. The fastest of all possible paths from a given structure type to the global minimum for landscapes of the glass dataset, and additional datasets containing outliers. The paths are shown as sequences of minima and transition states connected by straight lines. The minima lie at integer values on the x -axis.

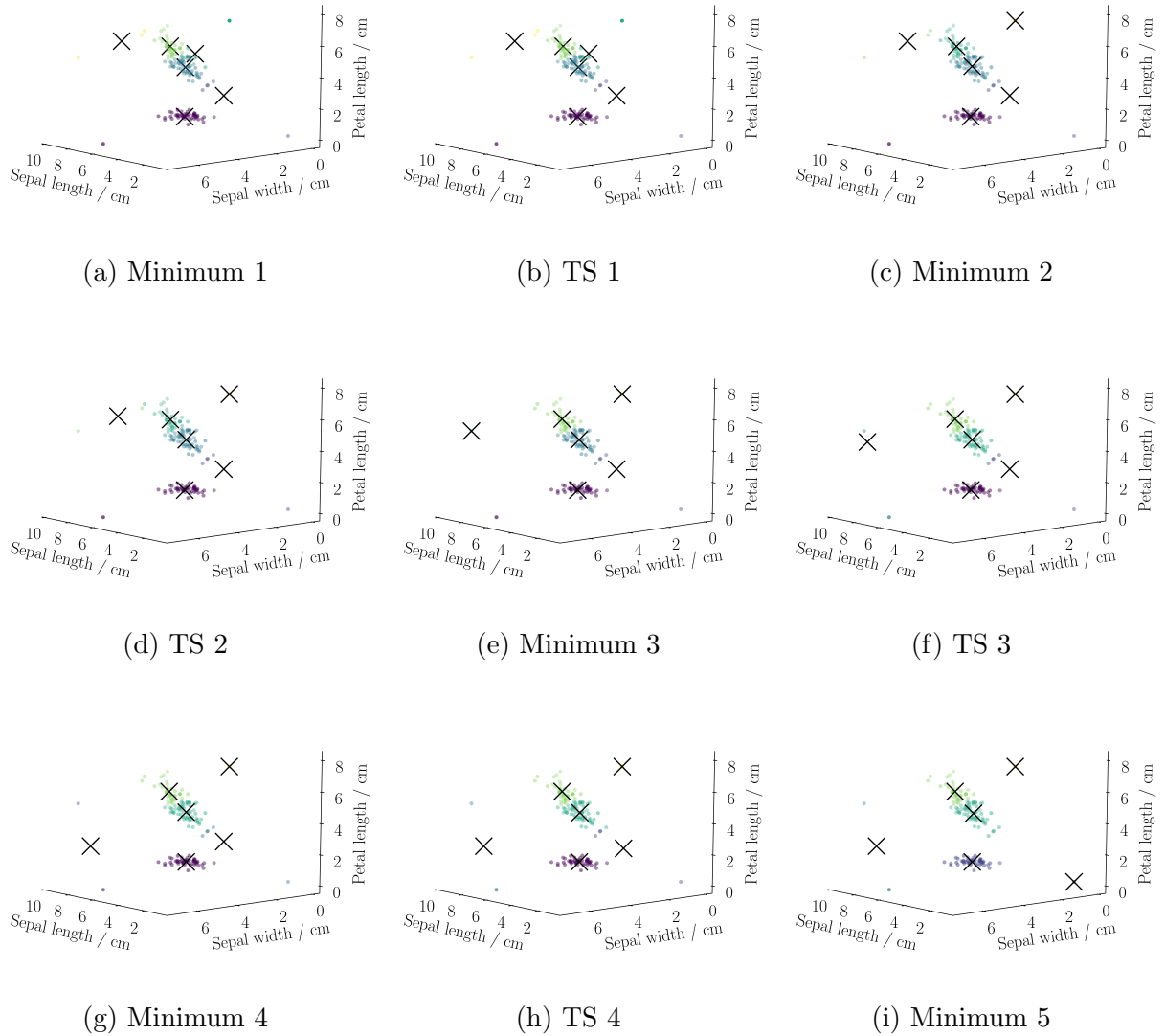


FIG. 2. Stationary points on the fastest path between all minima of structure type 0 and the global minimum of structure type 8 for the *Iris* dataset with $K = 6$ and four outliers. Each stationary point is visualised using three of the four features. This pathway requires three large structural changes to progress to the global minimum and, consequently, the rate is much lower than observed in landscapes with fewer outliers.

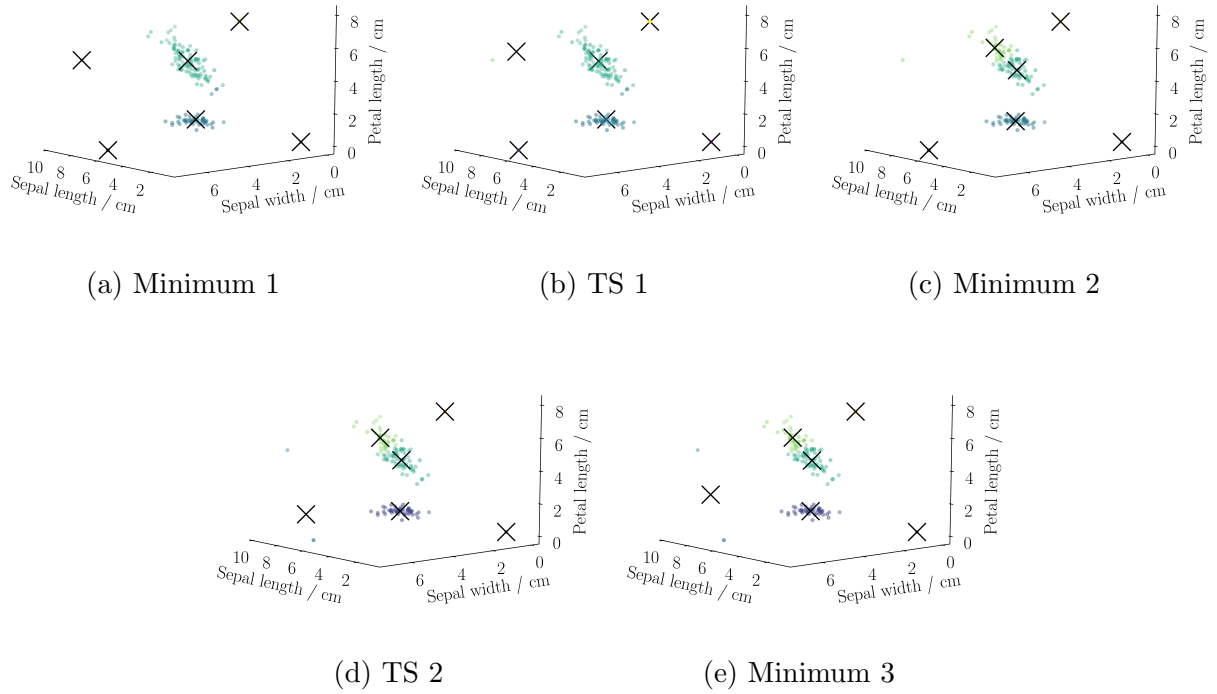
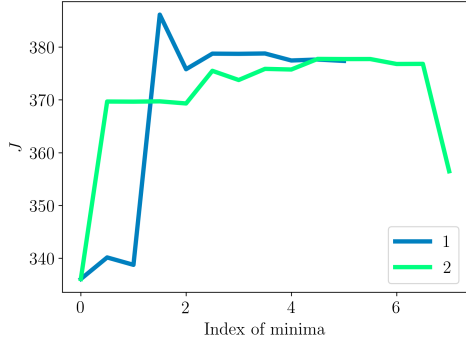
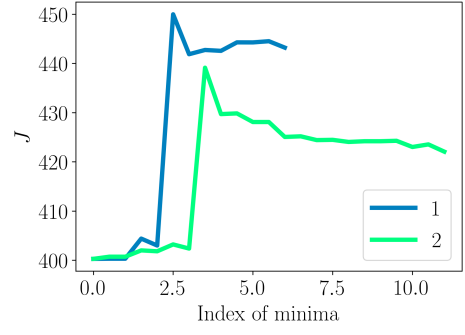


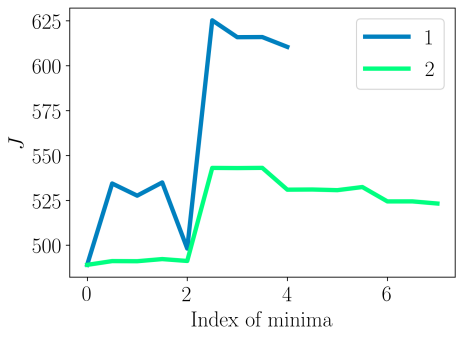
FIG. 3. Minima and transition states on the fastest path between the set of minima of structure type 7 and the global minimum of structure type 8 for the *Iris* dataset with six clusters and four outliers. The pathway retains a rate similar paths in the landscape with one outlier because of the similarity between the start and end minima. The similar structure types mean that less reorganisation is needed, and the transition can be achieved with fewer intermediate minima.



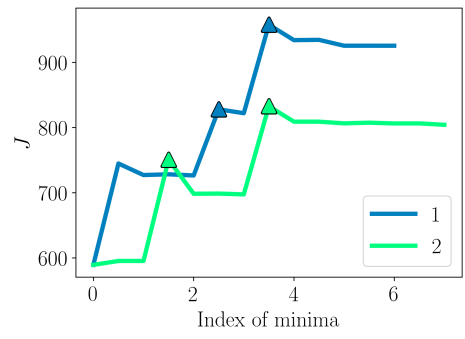
(a) Original



(b) Outlier 1



(c) Outlier 2



(d) Outlier 3

FIG. 4. Fastest paths from selected kinetic traps to the global minimum, for the K -means landscapes of the glass dataset and its variations. Paths are represented by minima and transition states, connected by straight lines. The minima lie at integer values on the horizontal axis and transition states give the cost function barrier between them. Changes in structure type are denoted by triangles placed on the transition state between the two differing minima.

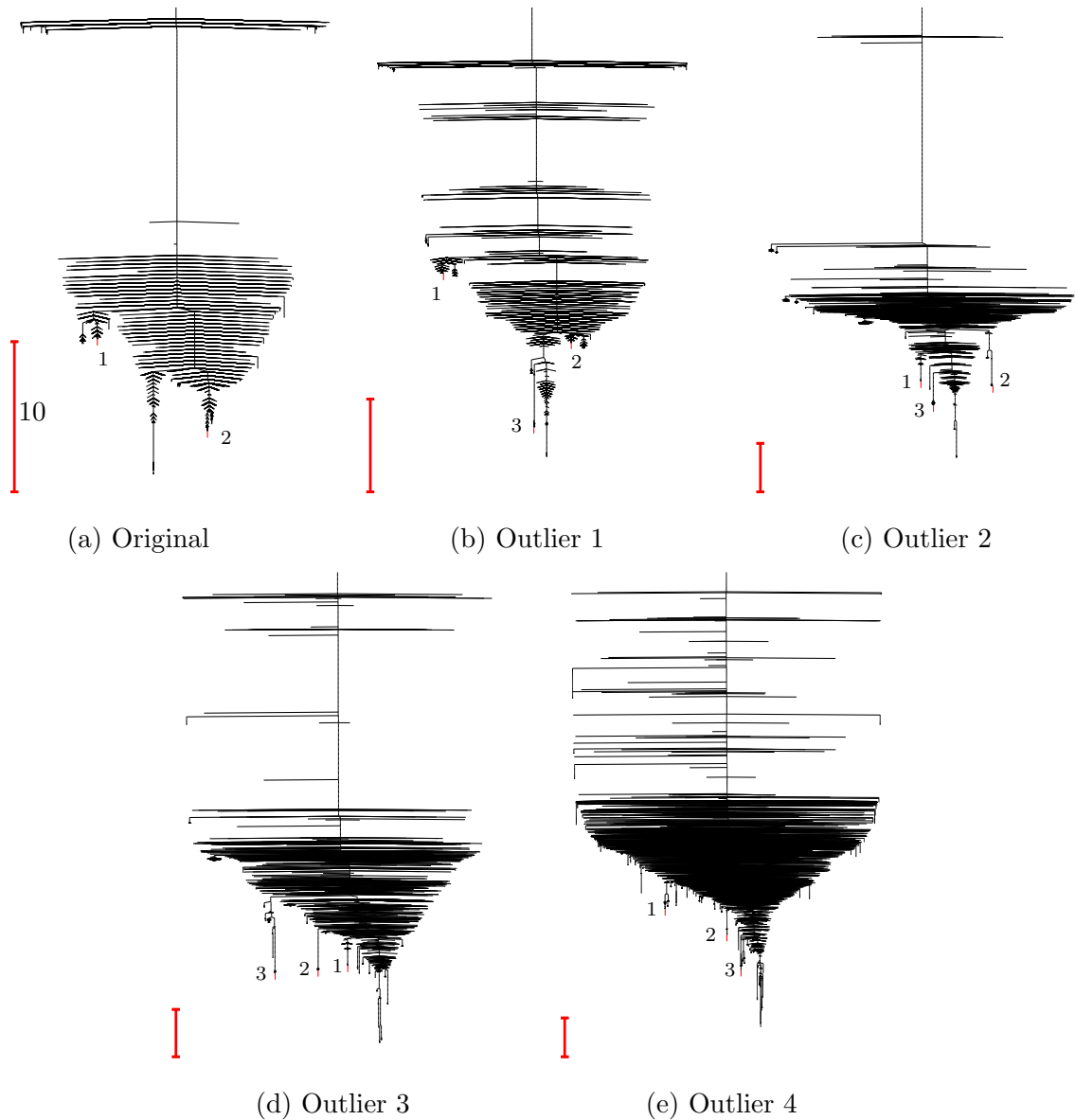


FIG. 5. K -means landscapes for Fisher’s *Iris* dataset with $K = 6$, highlighting kinetic traps. The lowest minimum from each kinetic trap is coloured red, and the associated numerical label is given. The numbering corresponds to that used in Sec. A.3 of the main text.

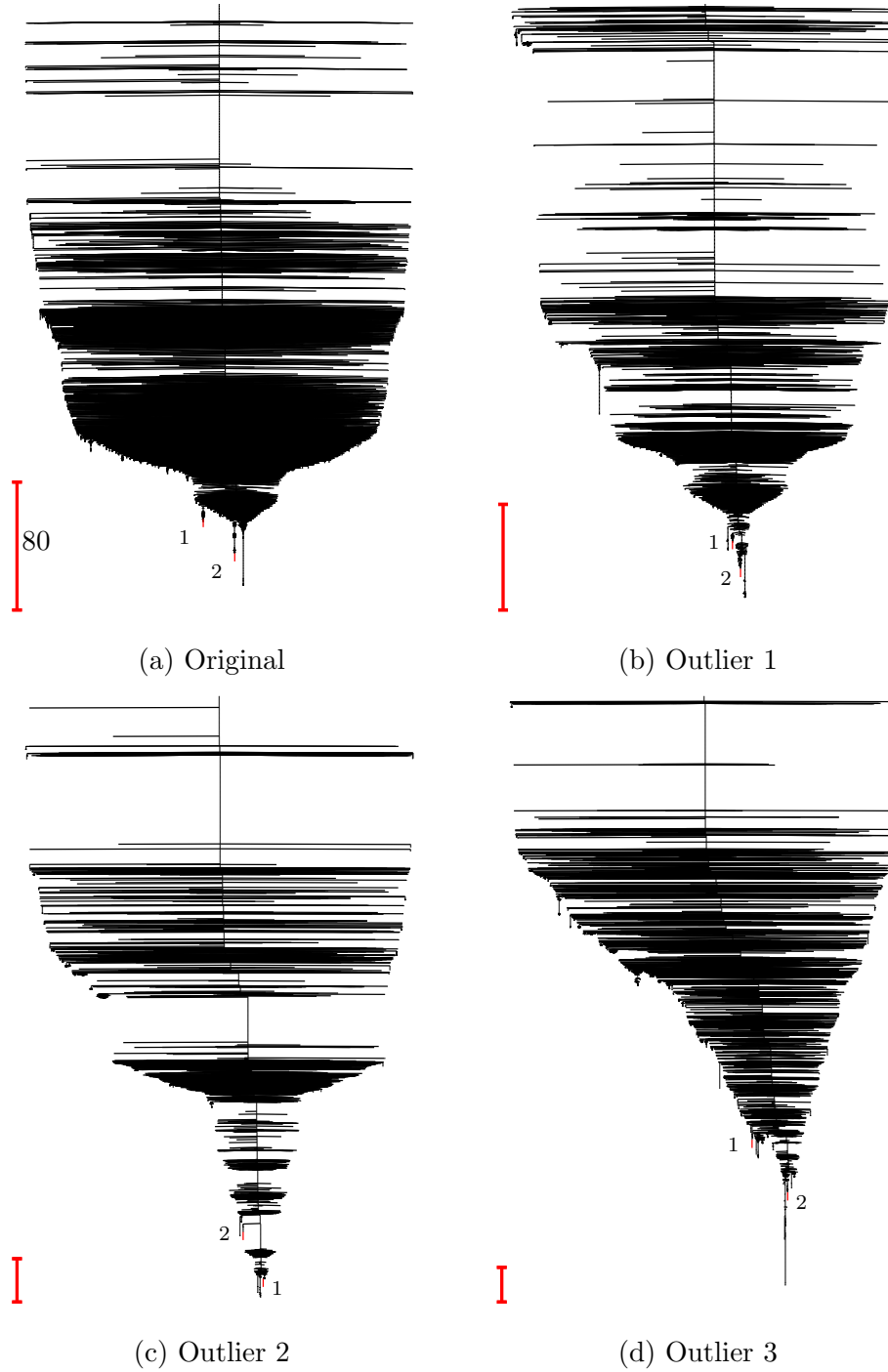


FIG. 6. K -means landscapes for the glass datasets with varying outlier number. Selected kinetic traps are identified by red minima in the disconnectivity graph, with the associated label. The label corresponds to the kinetic traps given in Sec. A.3 of the main text.

B. Clustering solution properties

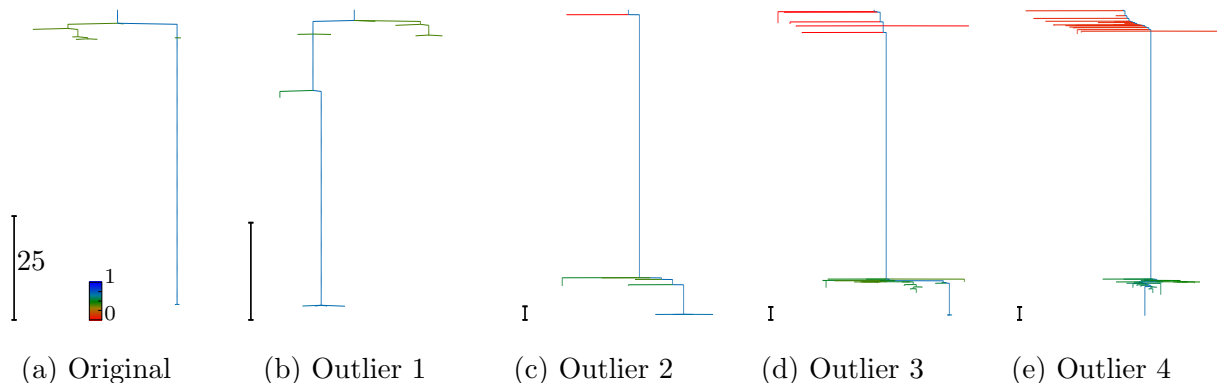


FIG. 7. Disconnectivity graphs for K -means landscapes of Fisher’s *Iris* dataset with $K = 3$ for the original dataset, and datasets with outliers. The minima are coloured according to the ARI relative to the ground truth labels. The scalebar and colour scale are the same for all panels in the same row.

TABLE III. The accuracy of clustering solutions in the glass landscapes. The highest achievable accuracy is given, along with the cost function gap between this clustering and the global minimum, and its structure type. The accuracy of the global minimum (GM) is also given, along with its structure type.

	Best accuracy	ΔJ	Type	Accuracy (G)	Type (GM)
Original	0.313	126.80	-	0.255	-
Outlier 1	0.303	24.04 / 180.66	1 / 0	0.252	1
Outlier 2	0.303	595.26	1	0.252	2
Outlier 3	0.299	811.15	3	0.226	4

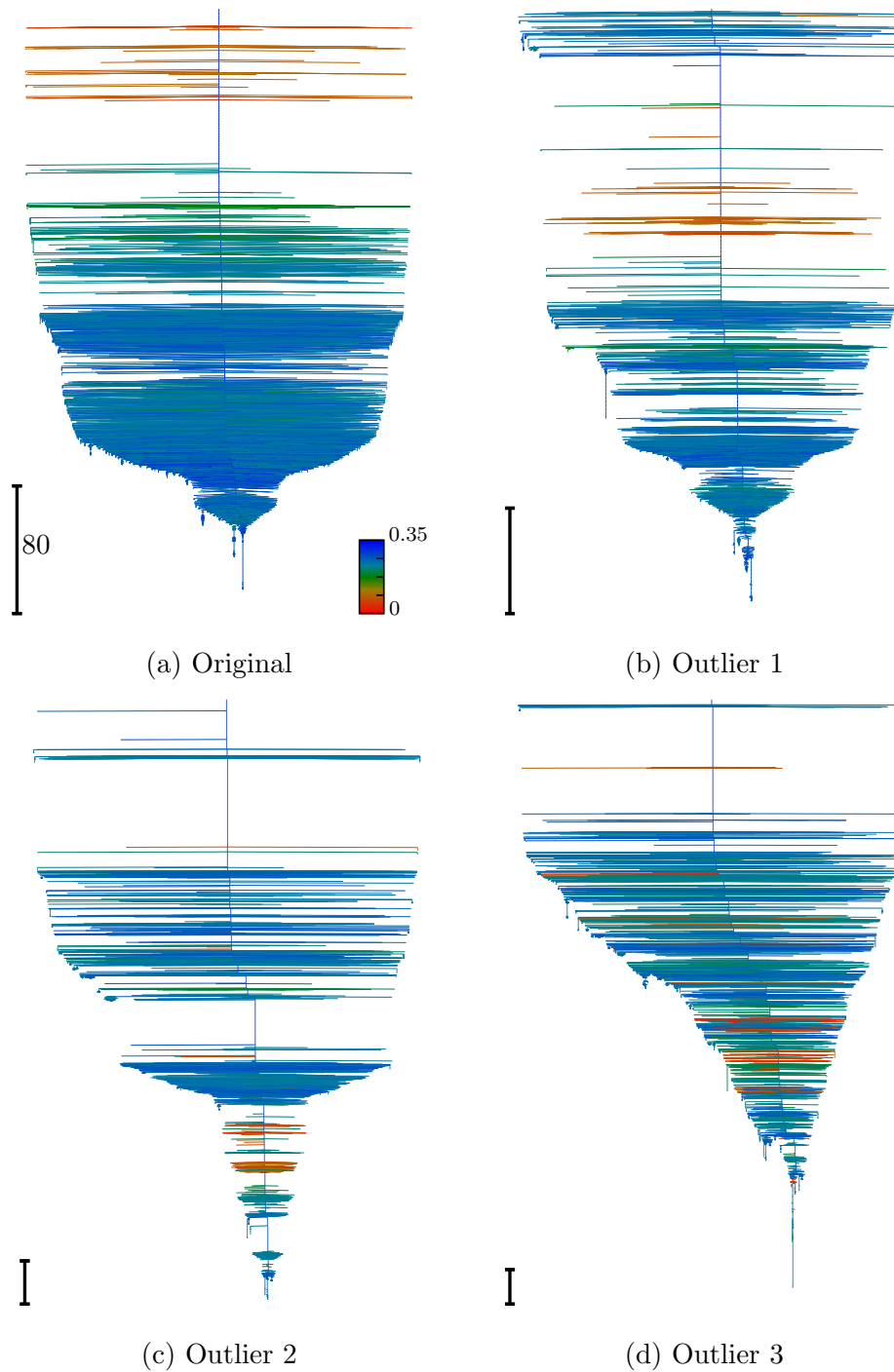


FIG. 8. Disconnectivity graphs showing the K -means landscapes for the glass datasets with an increasing number of outliers. The scale bar represents the same range in all plots. The colouring of minima is defined by the ARI between the cluster labels of each minimum and the ground truth labels. The colour range is given in (a) and remains the same in all plots.

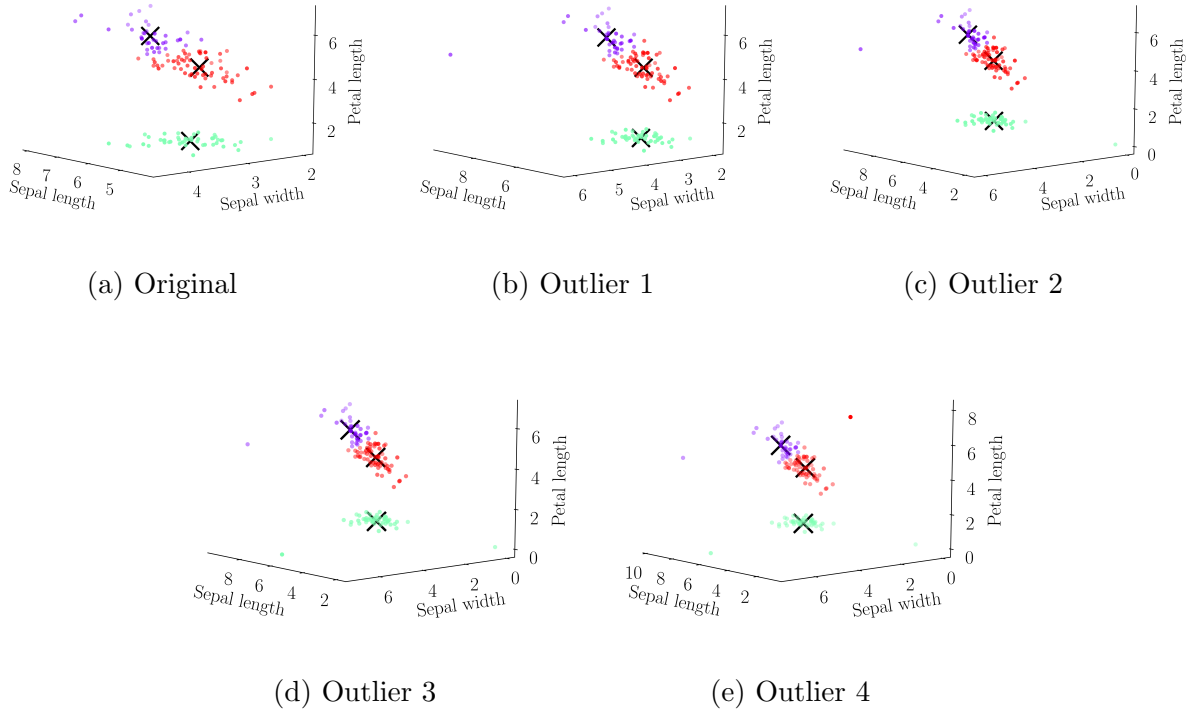


FIG. 9. Global minima for the *Iris* landscapes with $K = 3$. Three of the four features are presented to allow visualisation, given in centimetres. Petal width is excluded as it contains little information. Cluster centres are denoted by large black crosses, and the assignment of the data points to each of the three clusters is given by their colour.

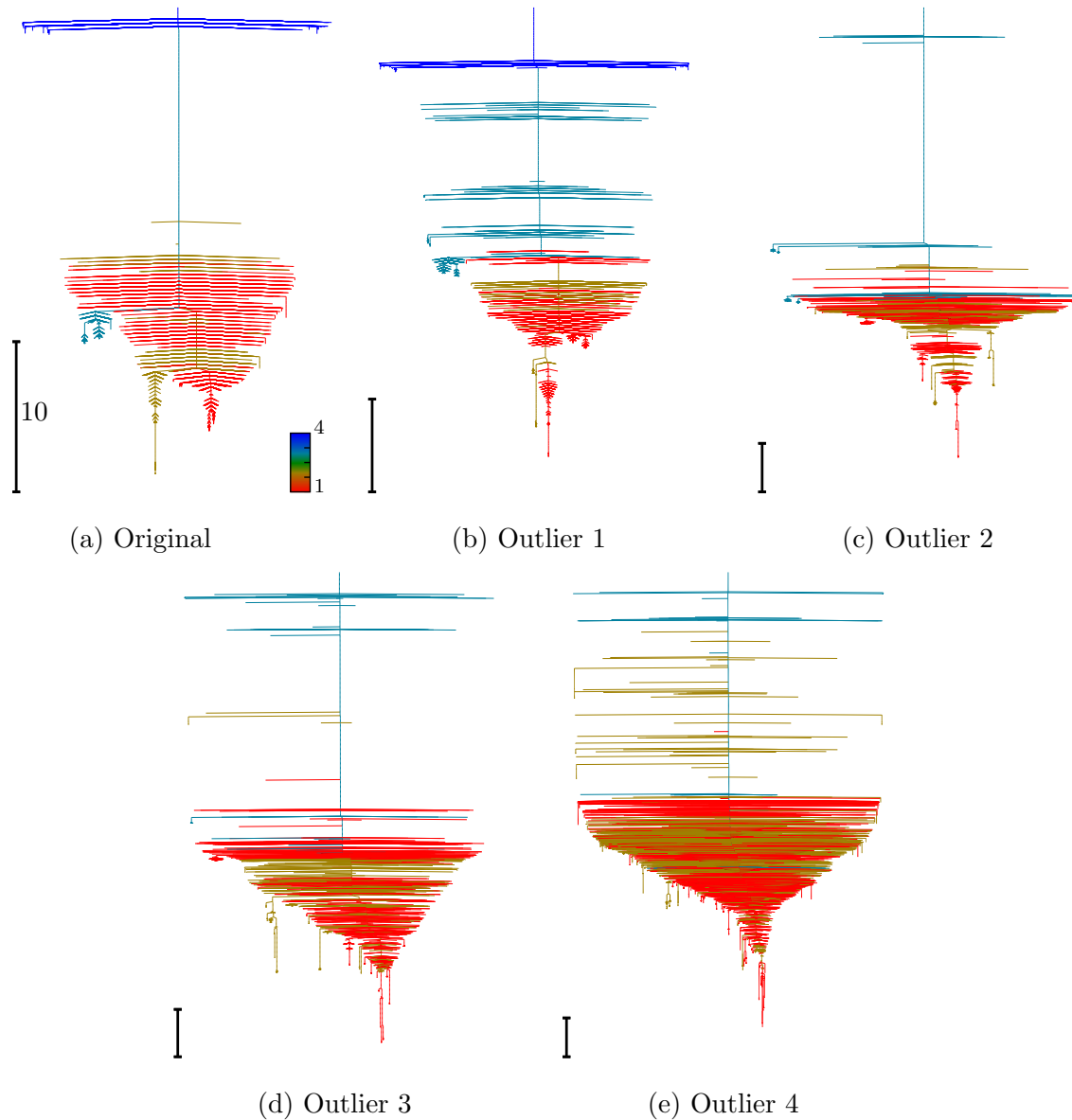


FIG. 10. Disconnectivity graphs for K -means landscapes of Fisher's *Iris* dataset with six clusters. Minima are coloured according to the number of clusters assigned to the *Setosa* data points. The cost function and colour scale are the same in all plots.

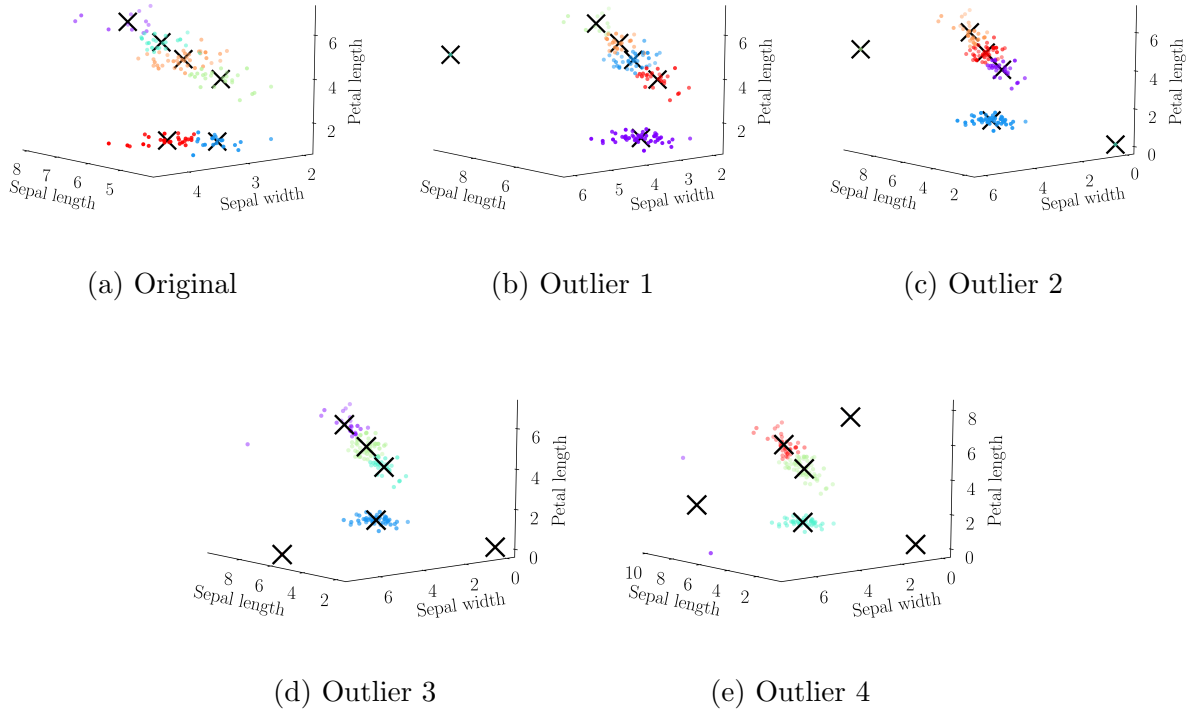


FIG. 11. Global minima for the *Iris* landscapes with $K = 6$, and a growing number of outliers. Minima are presented in three of the four features to allow visualisation, given in centimetres. Petal width is excluded as it contains the least information. The colours denote assignment to the cluster centres, which are denoted by black crosses.

V. RATE-BASED CLUSTERING COMPARISON

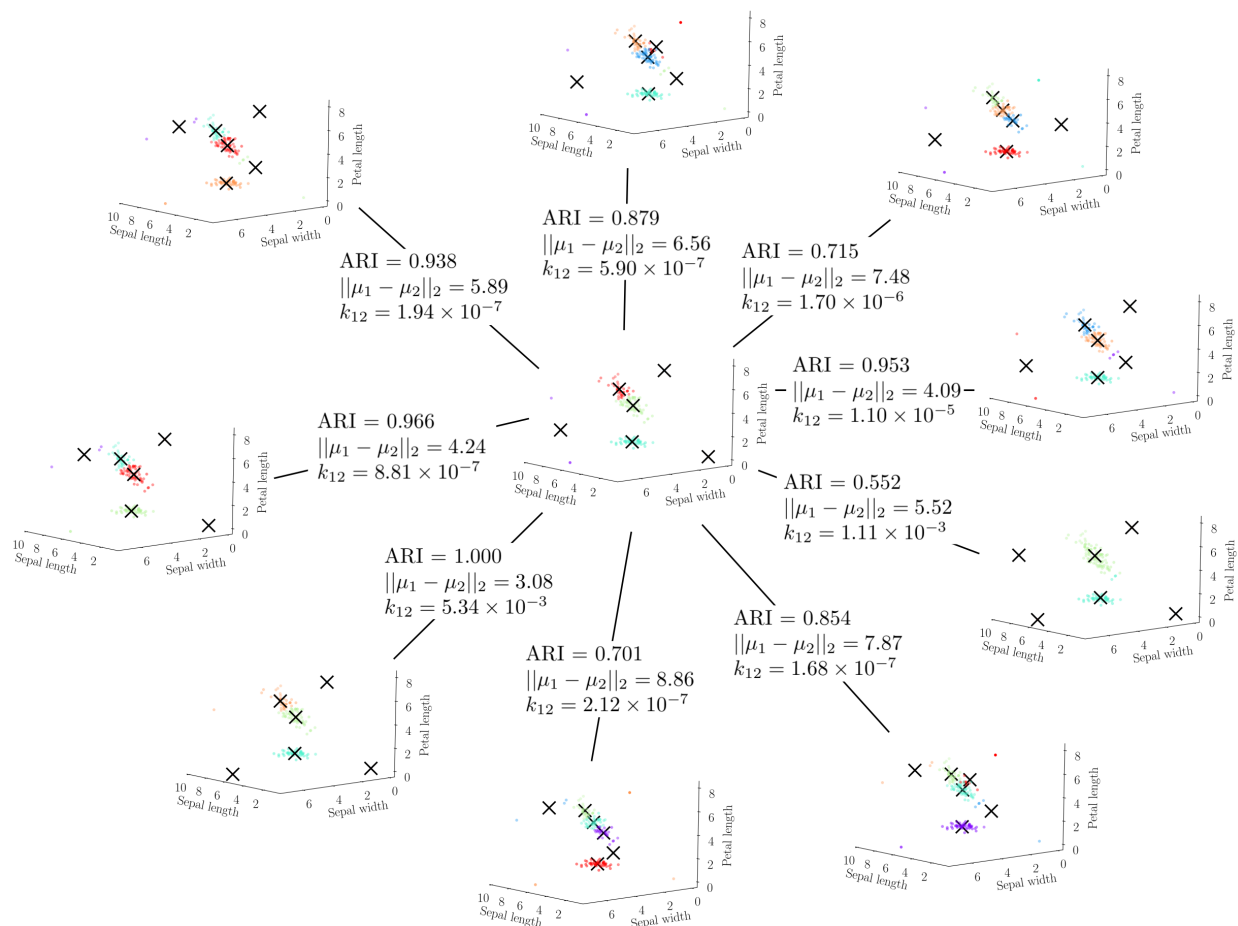


FIG. 12. The different structure types of clustering solution for the *Iris* dataset with four outliers. The value of the cluster comparison metrics are given for each minimum to the global minimum in the centre.

TABLE IV. Transition rates (reduced units) between the set of minima with a given structure type to the global minimum for the glass dataset, and variations with additional outliers. Rates are calculated at a fictitious temperature $T = 3.0$ in reduced units. The dot indicates the structure type of the global minimum.

Type	Outlier 1	Outlier 2	Outlier 3
0	2.54×10^{-4}	8.13×10^{-7}	2.17×10^{-10}
1	.	5.45×10^{-7}	2.45×10^{-10}
2		.	4.84×10^{-10}
3			2.92×10^{-11}
4			.
5			9.41×10^{-11}

TABLE V. Transition rates (reduced units) from minima at the bottom of kinetic traps to the global minimum for various K -means landscapes of the glass dataset. The rates are calculated for selected kinetic traps, which are shown in Fig. S6, at a fictitious temperature of $T = 3.0$. The geometric mean rate for each landscape is given in the final row.

Kinetic trap	Original	Outlier 1	Outlier 2	Outlier 3
1	1.77×10^{-5}	7.83×10^{-4}	2.49×10^{-6}	1.30×10^{-6}
2	8.25×10^{-6}	4.86×10^{-4}	3.55×10^{-6}	4.84×10^{-10}
Mean	1.21×10^{-5}	6.17×10^{-4}	2.97×10^{-6}	2.51×10^{-8}

REFERENCES

- ¹O. M. Becker and M. Karplus. The topology of multidimensional potential energy surfaces: theory and application to peptide structure and kinetics. *J. Chem. Phys.*, 106:1495–1517, 1997.
- ²W. M. Rand. Objective criteria for the evaluation of clustering methods. *J. Am. Stat. Assoc.*, 66:846–850, 1971.
- ³L. Hubert and P. Arabie. Comparing partitions. *J. Classif.*, 2:193–218, 1985.